Reviewed Preprint
v1 • September 29, 2025
Not revised

Reviewed Preprint
v2 • April 17, 2026
Revised by authors

Inverted Assembly of the Lens Within Ocular Organoids Reveals Alternate Paths to Ocular Morphogenesis

Elin Stahl[1,2,†], **Miguel Angel Delgado-Toscano**[1,3,†], **Ishwariya Saravanan**[1], **Anastasija Paneva**[1,2], **Joachim Wittbrodt**[1] ✉, **Lucie Zilova**[1,*] ✉

[1]Centre for Organismal Studies Heidelberg (COS), Heidelberg University, Heidelberg, Germany • [2]Deutsches Krebsforschungszentrum (DKFZ), Heidelberg, Germany • [3]Epigenetics and Neurobiology Unit, European Molecular Biology Laboratory (EMBL) Rome, Monterotondo, Italy

For correspondence:
jochen.wittbrodt@cos.uni-heidelberg.de
lucie.zilova@cos.uni-heidelberg.de

[†] these authors contributed equally

[*] Lead contact

Competing interests: No competing interests declared

Funding: See page 25

Reviewing editor: Filippo Del Bene, Institut de la Vision, France

eLife Assessment

This **important** study demonstrates that ocular organoids can generate both retina and lens through a non-canonical, "inside-out" morphogenetic route. The work is supported by **convincing** data, with well-designed experiments combining imaging, molecular analysis, and transcriptomics to establish that lens formation in organoids follows conserved molecular programs despite an alternative morphogenesis. These findings expand our understanding of self-organization and developmental plasticity, and will be of broad interest to researchers working on eye development, organoids, and tissue engineering.

[Editors' note: this paper was reviewed by *Review Commons*.]

https://doi.org/10.7554/eLife.108702.2.sa4

Abstract

The eye is a complex organ composed of two main structures – the retina and the lens. It forms by the invagination of the lens forming head surface ectoderm embedding into the forming optic cup. This “outside-in” mode of morphogenesis ensures that the light focusing lens is positioned centrally inside of the eye in the highly constrained environment of the developing embryo. Advances in stem cell biology in the last decade introduced organoids as model to study organogenesis under normal and diseased conditions. However, even though strikingly similar at some points, it remained elusive to which extend the generation of individual structural features in organoids recapitulates *in vivo* organogenesis. Here we describe the generation of fish ocular organoids composed of both, lens and retina, using pluripotent embryonic cells from medaka (*Oryzias latipes*). Formation of the organoid lens followed the key molecular features of the process *in vivo*, including the establishment of lens progenitor cells and their subsequent differentiation into lens fiber cells. In a process dependent on the coordinated activity of BMP and FGF signaling, lens formation in ocular organoids was marked by the expression of key genes implicated in organismal lens development. Despite adhering to the basic molecular machinery of lens formation *in vivo*, the morphogenesis into a spherical lens followed an “inside-out” mode. Lens progenitor cells were initially established and differentiated into a spherical lens directly inside of the retina. Subsequent displacement of the lens from the center of the organoid towards its surface ultimately led to the formation of a cup-like shaped retina with a centrally positioned lens. Our study highlights that the self-organization of the organoid can favor routes that were not selected for in the developing embryo. Those routes can lead to an alternative, though highly similar outcome with the respect to achieving specific structural features in an unconstrained, embryo-free environment.

Introduction

The tissues of the embryo develop in an evolutionarily selected confined space with robust physical and biochemical constraints. Precise spatio-temporal gradients of growth factors aligned with complex mechanical forces guide cell and tissue interactions, permitting the coordinated formation of functional tissues and organs. Eye development is an example of complex organ formation relying on the coordinated interactions of tissues of different embryonic origin. This ultimately results in the positioning of a light-focusing lens in the center of the light-sensing retina (Cardozo et al., 2023; Casey et al., 2021; Chow and Lang, 2001; Cvekl and Ashery-Padan, 2014).

While the lens originates from the head surface ectoderm (SE), the retina originates from optic vesicle (OV), a lateral evagination of the forming diencephalon. In vertebrates, eye development is initiated at the end of gastrulation when the anterior ectoderm is patterned into the neural plate, non-neuronal ectoderm and the neural plate border at their interface. Lens-committed progenitors are first found in the anterior neural plate border, also called the anterior pre-placodal region (Bailey and Streit, 2005; Bhattacharyya et al., 2004; McCabe and Bronner-Fraser, 2009; Schlosser, 2006; Toro and Varga, 2007). Retina-committed progenitors, on the other hand, are established within the anterior neural plate, by the specification of the eye field, followed by the evagination of the optic vesicle (Adelmann, 1937; Eagleson et al., 1995; Kenyon et al., 2001; Li et al., 1997). Once the retina-forming OV contacts the lens-competent ectoderm, interactions of OV, SE and the surrounding tissues result in the formation of the lens placode within the head surface ectoderm. The concomitant invagination of lens placode and morphogenesis of the OV then lead to the formation of the lens vesicle in the center of the forming optic cup (Casey et al., 2021; Chow and Lang, 2001; Cvekl and Ashery-Padan, 2014; Gunhaga, 2011). Initially the lens vesicle is composed of lens progenitor cells. It is further patterned into lens epithelium at the anterior part of the lens, while posteriorly located progenitors differentiate into lens fiber cells (Kallifatidis et al., 2011; Zhou et al., 2006). The differentiation of lens fiber cells is characterized by the production and accumulation of crystallin proteins, the main structural proteins of the lens (Cvekl et al., 2015; Donaldson et al., 2017). This transition is marked by the extensive elongation of cells (Cheng et al., 2017; Fudge et al., 2011; Rao and Maddala, 2006) and the subsequent degradation of all organelles and de-nucleation (Bassnett, 2009; Brennan et al., 2021; Chaffee et al., 2014; Wride, 2011), minimizing light scattering and providing optimal refractive properties, all together resulting in the optical properties of the lens (Bassnett et al., 2011).

Several studies have shown that the conserved process of lens formation depends on the intricate interplay of intrinsic factors and extracellular signalling pathways (Cvekl and Ashery-Padan, 2014; Cvekl and Zhang, 2017; Lang, 2004; McAvoy et al., 1999; Ogino and Yasuda, 2000). The transcription factors *Pax6*, c-*Maf*, *Sox1*, *Prox1*, *Hsf4*, *Six3*, *Foxe3*, *Pitx3*, *Sox2* characterise early lens development and are directly involved in the processes of initial lens morphogenesis and lens fiber cell differentiation (Cvekl and Duncan, 2007; Cvekl and Zhang, 2017; Lang, 2004; Ogino et al., 2012; Ogino and Yasuda, 2000). Establishment of lens-competent progenitors as well as differentiation of lens fiber cells relies on the interplay of the FGF, BMP, and WNT signalling pathways (Faber et al., 2001, 2001; Furuta and Hogan, 1998; Grocott et al., 2011; Gunhaga, 2011; Jarrin et al., 2012; Kreslova et al., 2007; Le and Musil, 2001; Litsiou et al., 2005; Lovicu and McAvoy, 2005; McAvoy et al., 1999; Rajagopal et al., 2009).

Although many aspects of lens formation are well characterized, addressing the molecular mechanisms in the complex environment of the developing embryo is often challenging. Advances in stem cell and developmental biology allowed the introduction, fast development and prominent use of organoids as new models to study complex processes of *ex vivo* organ formation. Those allow to gain insight into cellular and molecular processes in normal and diseased conditions in a controlled and experimentally accessible *in vitro* environment (Chen et al., 2024; Hofer and Lutolf, 2021; Kretzschmar and Clevers, 2016; Sahu and Sharan, 2020; Zhao et al., 2022).

Mouse, human and fish pluripotent embryonic stem cells have been shown to self-organise into retinal tissue when aggregated and cultured under minimal growth factor 3D suspension culture conditions. Retinal organoids recapitulate key aspects of embryonic development with respect to cell fate commitment, tissue patterning, cell differentiation and physiological functions (Eiraku et al., 2011; Kuwahara et al., 2015; Nakano et al., 2012; Völkner et al., 2016; Zilova et al., 2021). Since the culture conditions for the generation of retinal organoids favor neuroectodermal differentiation over non-neuronal ectodermal fates, they did so far not allow for concomitant lens formation (Eiraku et al., 2011; Kuwahara et al., 2015; Nakano et al., 2012; Zilova et al., 2021).

Generation of lens-like structures (lentoid bodies) by stepwise differentiation of human ES or iPS cells has been reported (Cvekl and Camerino, 2022; Dincer et al., 2013; Fu et al., 2017; Leung et al., 2013; Yang et al., 2010). However, most lens differentiation protocols directly favor the promotion of placodal fate on the expense of the neuronal fate (Dincer et al., 2013; Fu et al., 2017; Yang et al., 2010). This rendered the generation of more complex organoids composed of cell types of diverse embryonic origin challenging. Interestingly, two independent studies had reported the appearance of lens marker-expressing cells in close vicinity to retina tissue in 3D organoid culture (Gabriel et al., 2021; Mellough et al., 2015). However, considering the complex nature of tissue interactions required for the coordinated formation of both lens and retina *in vivo*, this raises the intriguing question of how a lens is formed in neuronal organoids and to what extend that process recapitulates *in vivo* organ formation.

Here we used organoids derived from *Oryzias latipes* blastula cells as a model system to investigate the formation of ocular organoids composed of both, retina and lens. By following the individual populations of lens- and retina-committed progenitors, we found that similar to the *in vivo* situation, lens and retina originate from spatially confined and separated populations of progenitor cells. The subsequent differentiation into their respective lineages was found to be dependent on BMP and FGF signaling pathways. Their differentiation and morphogenesis are characterized by the expression of key regulatory factors implicated in eye (lens and retina) organogenesis, however following an entirely different morphogenetic route towards forming an eye cup enclosing a centrally positioned lens.

Results

Fish retinal organoids form embedded lenses under specific culture conditions

We have previously reported the generation of retinal organoids from fish pluripotent embryonic cells grown in 3D suspension culture in minimal growth factor-containing media. Such organoids acquire anterior neural fate and consist of retina and presumptive forebrain tissue (Zilova et al., 2021). Here, we modified our previously described protocol (Figure 1a) in order to generate organoids, that differentiated into retinal and lens tissues.

Aggregation of fish primary pluripotent cells in DMEM/F12-based differentiation media supplemented with 5% knockout serum replacement and 20 mM HEPES pH 7.4 (see Materials and Methods for detailed composition) resulted in the efficient formation of retinal organoids containing a single transparent, spherical lens-like structure surrounded by neuronal tissue (Figure 1b). The lens-like structure was clearly visible at day 4 but first signs of its formation could be observed from day 2 onwards (Figure 1b, asterisk). We showed that organoids were composed of both retina and lens tissue, arranged in a way that was reminiscent of the tissue arrangement in the embryonic eye by using reporter lines and molecular markers. Differentiated lens cells expressing crystallin were labelled in the *Gaudi*^{RSG} transgenic reporter line (Centanin et al., 2014) that carries a *crystallin::ECFP* (*Cry::ECFP*) reporter. Lens fiber cells were identified with the “lens fiber cell” marker antibody ZL-1 (referred to as LFC), and early and late lens cells were identified with an anti-Prox1 antibody (Figure 2a and 2b). Prox1 is expressed by cells of the lens placode and differentiating lens fiber cells of different species including mouse, zebrafish and medaka (Mikula Mrstakova and Kozmik, 2024; Pistocchi et al., 2008; Wigle et al., 1999).

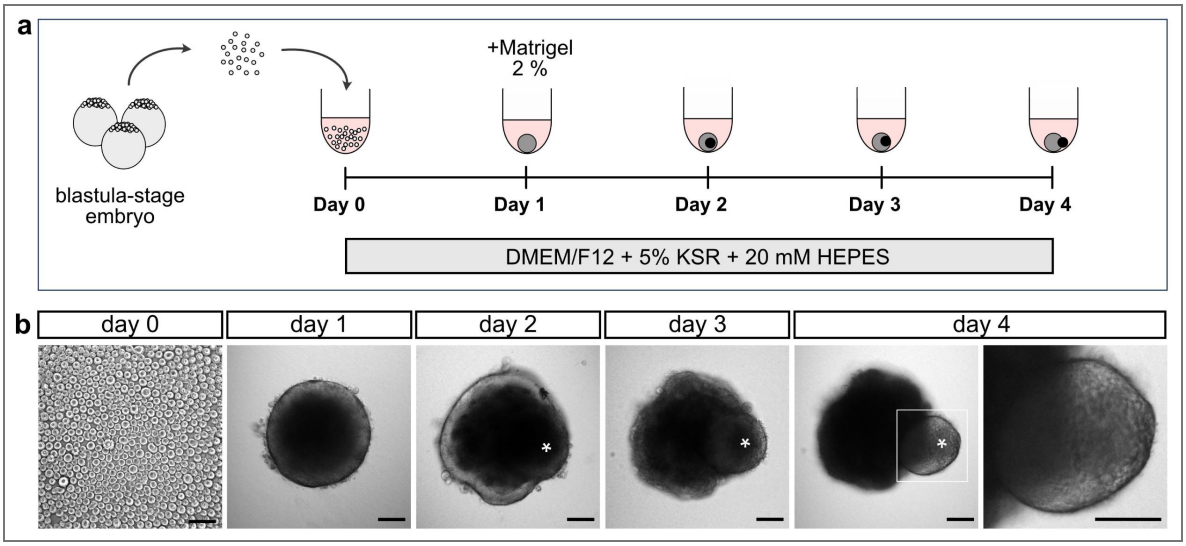

Figure 1. Generation of organoids from medaka pluripotent embryonic cells.

(a) Schematic representation of organoid generation. At day 0, pluripotent embryonic cells were extracted from blastula-stage medaka embryos and seeded in U-bottom, low-binding 96-well plate into DMEM/F12 media supplemented with 5 % KSR and 20 mM HEPES pH 7.4. At day 1 aggregates were supplemented with 2 % Matrigel. **(b)** Bright-field pictures of indicated stages of organoid formation showing the appearance of lens-like structure (asterisk). KSR, knockout serum replacement. Pictures acquired with wide-field microscope (Mi8; Leica). Scale bar 100 µm.

Anti-LFC labels lens fiber cells in zebrafish and is suggested to target one of the crystallin proteins (Greiling et al., 2010; Shi et al., 2006). In the medaka embryo, the expression of both, crystallin promoter-driven ECFP and LFC marker was observed exclusively in the lens 3 days post-fertilization (dpf) (Figure 2a). Prox1 immunolabeling was detected in the lens and a subpopulation of differentiating retinal cells in the central region of the retina (Figure 2a). The expression of all three lens markers was detected in day 4 ocular organoids (Figure 2b and 2c), demonstrating that the spherical structure formed by the organoids is indeed the lens. ECFP labeling was sparse (25 % *Cry::ECFP*, Figure 2b) reflecting the mode of generation of the organoids by a combination of 25 % cells carrying the *Cry::ECFP* reporter and 75 % wild-type cells (see Materials and Methods for details).

The transgenic reporter lines *Atoh7::EGFP* (Del Bene et al., 2007) and *Rx3::H2B-GFP* (Rembold et al., 2006) were used to identify retinal tissue in lens carrying organoids. In embryos *Atoh7::EGFP* activity was confined to the retina, labelling differentiating retinal neurons at 3 dpf (Figure 2a). In organoids, labeled retinal cells surrounded the forming lens, reminiscent of the situation in the eye. To address the distribution of retinal and lens cells we used blastula cells from *Atoh7::EGFP* and *Rx3::H2B-GFP* retina-specific reporter lines (Figure 2d and 2e) and co-labeled *Rx3::H2B-GFP*-derived day 4 organoids with anti-LFC antibody (Figure 2e).

Analysis of the organoid lens revealed a great similarity with structural features of the developing embryonic lens, such as the elongation of $Prox1^{+}/LFC^{+}$ cells, typical for differentiating lens fiber cells and atypically looking nuclei indicating disorganization of nuclear material, a process tightly connected to lens fiber cell differentiation (Figure 2b and 2h, arrowhead).

In 462 organoids derived from 38 independent experiments we observed lens formation, in 83.5 % (n=386) of organoids. A careful evaluation of different culture conditions and their impact on the lens formation revealed that lens formation depends on supplementation of the DMEM/F12-based differentiation media with 20 mM HEPES buffer (Figure 2-figure supplement 1a and 1b). While organoids grown without HEPES supplementation never formed lenses (n=63 organoids in 6 independent experiments, see also Zilova et al., 2021), 92 % of organoids grown in media supplemented with HEPES (n=83 organoids in 6 independent experiments) formed lenses (Figure 2-figure supplement 1b).

We tested the impact of extracellular matrix (ECM) supplementation on lens formation, as existing protocols for generation of lentoid bodies from human pluripotent embryonic stem cells mostly rely on supplementation with ECM proteins (Dincer et al., 2013; Fu et al., 2017; Leung et al., 2013; Yang et al., 2010), usually in form of Matrigel. Interestingly, lens cell fate specification as well as lens fiber cell differentiation, judged by the expression of Prox1 and LFC, occurred independently of Matrigel (2 % final concentration) supplementation in medaka-derived organoids (Figure 2-figure supplement 1d and, f). Matrigel impacted mostly on the organization and thickness of $Rx2^{+}$ retinal neuroepithelium localized on the surface of the organoids (Figure 2-figure supplement 1c). Measurement of the size of the lens (diameter of LFC^{+} lens sphere) at day 2 and day 5 showed that Matrigel supplementation did not impact the size of the lens (Figure 2-figure supplement 1d-e) or its overall organization analyzed by immunolabeling (Prox1, LFC, DAPI) at day 4 (Figure 2-figure supplement 1f).

The lens originates from a spatially distinct population of placodal progenitors located in the central region of the organoid

We further investigated the origin of lens cells and how its formation compares to lens development *in vivo* in the developing organism. In the embryo, the lens originates from the lens competent head surface ectoderm (SE, magenta), which directly abuts the evaginating optic vesicle (OV, prospective retina, green) (Figure 3a). OV and SE invaginate in a coordinated way to form a lens sphere surrounded by the retina. In medaka embryos, those processes occur between 1 dpf and 2 dpf (Figure 3a, 3b). Concomitant with the completion of lens formation, the differentiation of lens fiber cells is initiated and marked by the expression of crystallin proteins (LFC; cyan) (Figure 3b). To track the distribution of lens and retinal progenitors, we generated

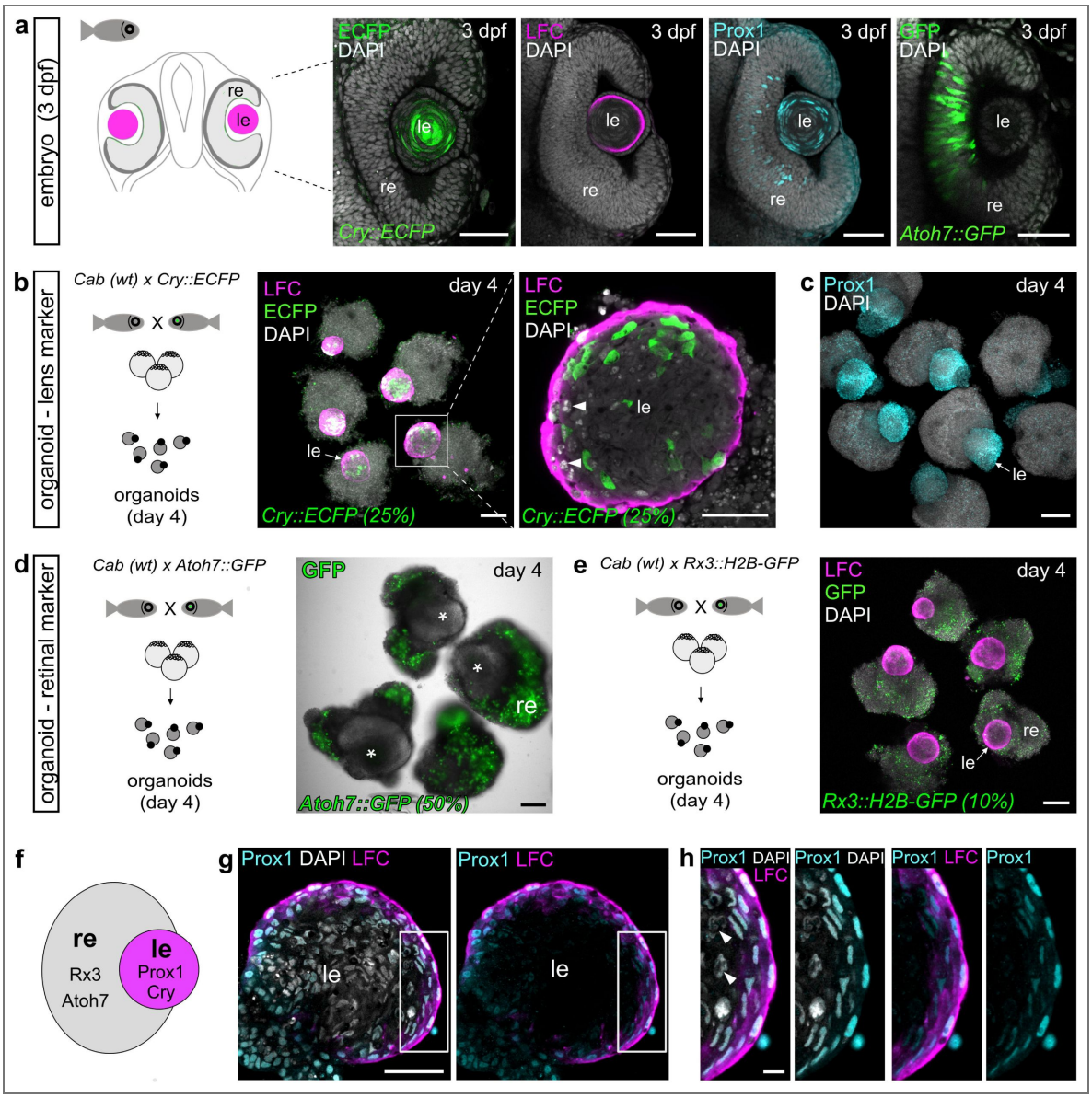

Figure 2. **Fish retinal organoids form lenses.**

(a) Expression of lens-specific markers (*Cry::ECFP*, lens fiber cell (LFC) and Prox1) and retina-specific marker (*Atoh7::EGFP*) in medaka embryonic eyes at 3 dpf. Optical sections showing the expression of indicated markers detected by whole-mount immunohistochemistry with the use of anti-GFP (green), anti-LFC (magenta) and anti-Prox1(cyan) antibodies, co-labelled with DAPI nuclear stain (grey). **(b)** Organoid generation from crystallin reporter line (*Cry::ECFP*). Expression of lens-specific markers (*Cry::ECFP* and LFC) in day 4 organoids detected by anti-GFP and anti-LFC antibodies. Represented by maximal projection for overview and single optical section for the detail of the lens. **(c)** Expression of Prox1 in day 4 organoids derived from wild-type medaka cells detected with anti-Prox1 antibody, co-stained with DAPI nuclear stain; displayed as maximal z-projection. **(d)** Organoid generation from retina-specific reporter line (*Atoh7::EGFP*). Overlay of bright-field and wide-field images showing EGFP fluorescence in *Atoh7*-expressing cells, lens indicated with asterisk. **(e)** Organoids generated from retina-specific reporter line (*Rx3::H2B-GFP*) labeled with anti-GFP and anti-LFC antibody displayed as maximal z-projection. **(f)** Schematic representation of distribution of retina- and lens-specific markers in day 4 organoids. **(g)** Optical section of day 4 organoid lens labeled with anti-Prox1 and anti-LFC antibodies, co-labeled with DAPI, showing elongated Prox1^{+}/LFC^{+} cells on the surface of the lens. **(h)** Enlargement of indicated area in g. For *Cry::ECFP*, *Atoh7::EGFP* and *Rx3::H2B-GFP*. The percentage (%) indicates how many cells carry the indicated transgene. Arrow in b, c and e indicates position of the lens. Arrowheads in b and h indicate abnormally looking nuclei. le, lens; re, retina; wt, wild-type; LFC, lens fiber cell. Scale bar 50 µm in a, g and enlargement of b, 100 µm in b-e, 10 µm in h.

organoids from the *Rx3::H2B-GFP* reporter line, which highlights retina-committed cells by nuclear GFP expression (Figure 3-figure supplement 1a and b). To visualize lens-committed progenitor cells within the SE (Mikula Mrstakova and Kozmik, 2024), we co-labeled those organoids with an anti-Prox1 antibody (Figure 3-figure supplement 1b) and followed the expression of *Rx3*-specific GFP and Prox1 from day 1 to day 2 (Figure 3c). Retinal progenitor cells were distinctly localized in the cortical region around the surface of day 1 organoids (Figure 3-figure supplement 1d, Figure 3c, Video S1), while lens progenitors (expressing Prox1) were not detectable at this stage (Figure 3c). Expression of retinal markers was confined exclusively to the cortex and was never detected in the central part of the organoid (Figure 2b, Figure 3-figure supplement 1d, Video S1). From day 1.5 onwards (stage S22 - 1 day and 14 h) (Iwamatsu, 2004), embryos as well as organoids (30 hours post aggregation) started expressing Prox1 (Figure 3b and 3c). In the embryo, Prox1 expression was localized to the surface of the head, labeling the presumptive lens region (Figure 3b). In the organoid, the expression was confined to the central core of the organoid with $Prox1^{+}$ cells organized into a sphere (Figure 3c). Prox1 expression in the central core of the organoids was followed by the expression of lens fiber cell differentiation marker LFC at day 2, concomitant with the onset of Prox1 and crystallin expression in the embryo (Figure 3b and 3c).

To specifically address the dynamics, onset, and cellular re-arrangements of lens-committed progenitors, we generated a *Foxe3::GFP* reporter line. *Foxe3* (winged helix/forkhead domain transcription factor) is necessary for proper lens development and is expressed by the cells of the presumptive lens ectoderm and lens epithelium of different species, including medaka (Blixt et al., 2000; Brownell et al., 2000; Mikula Mrstakova and Kozmik, 2024; Shi et al., 2006). This pattern is fully recapitulated by *Foxe3::GFP* with an onset of expression starting at 1 dpf (already in the presumptive lens ectoderm at stage S19 prior to lens placode formation at stage S21 where it is prominently expressed; Iwamatsu et al., 2004). It was further expressed by the majority of lens cells at 2 dpf, (Figure 3d) where it preceded the expression of the lens fiber cell marker LFC (Figure 3-figure supplement 2a). During development, the lens is composed of anteriorly located lens epithelium (proliferative lens progenitors) and posteriorly and centrally located differentiating lens fiber cells (Greiling et al., 2010). We could differentiate those parts of the developing lens with *Foxe3::GFP* expression in both, lens fiber cells and lens epithelium in 3 dpf embryo, and the expression of Prox1 and LFC restricted to differentiating fiber cells, but excluded from the lens epithelium (Figure 3-figure supplement 2a, arrows). Analysis at later stages showed that at 4 dpf, *Foxe3::GFP* expression was maintained in the lens epithelium (proliferatively active progenitors) and was nearly undetectable in differentiated lens fiber cells (Figure 3-figure supplement 2b, arrows).

In organoids, lens progenitor cells expressing *Foxe3::GFP* were first found in the central core at day 1 (26 hours post aggregation) (Video S2, Figure 3e, Figure 4, Video S3). These cells appeared in a pattern complementary to the retinal marker *Rx3::H2B-GFP* (Video S1), indicating that lens progenitor cells originate from a spatially distinct population in the central core of the organoid. We never detected any *Rx3*-positive cells eventually acquiring a lens fate. To address the distribution of lens and retina domains, we generated organoids from mixed blastula cells derived from the retina-specific reporter line *Rx2::H2B-RFP* (Inoue and Wittbrodt, 2011) and the lens specific reporter line *Foxe3::GFP* (Figure 3-figure supplement 2c). By day 2, lens progenitor cells expressing *Foxe3::GFP* contributed to the formation of a spherical lens in the central core of the organoid surrounded by unlabeled cells and eventually by the cortical retinal tissue (Figure 3g, Video S4).

Further analysis showed that the organoid lens consists of proliferating as well as differentiating cells (Figure 3-figure supplement 2d and e), however not localized to distinct domains as in the embryo. We found that *Foxe3*-driven GFP was co-expressed with the LFC differentiation marker in day 2 organoids (Figure 3-figure supplement 2e). EdU incorporation also showed that the lens is formed by proliferative (EdU^{+}) *Foxe3::GFP*-expressing cells (Figure 3-figure supplement 2d). On the surface of day 2 organoid lenses, we initially detected stretches of $Foxe3^{+}/LFC^{-}$ cells, reminiscent of the lens progenitor cells of the lens epithelium (Figure 3-figure supplement 2e

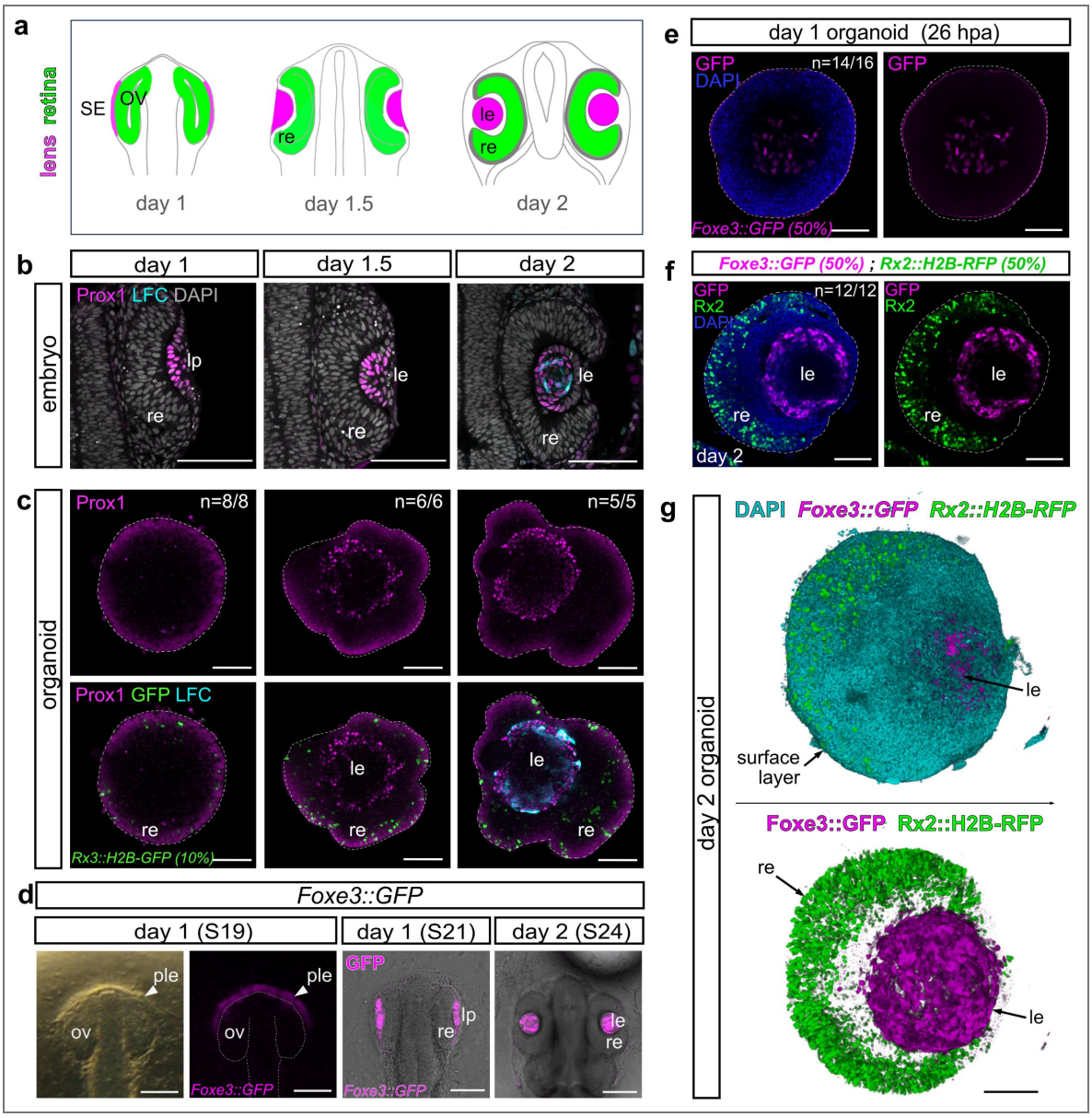

Figure 3. The lens originates from a spatially separated population of lens progenitors in center of the organoid.

(See also Figure S2 and S3, Video S1, S3 and S4.) **(a)** Schematic representation of lens formation in medaka. The lens develops from lens-competent head surface ectoderm (SE, magenta), retinal cells from the OV (green). Surface ectoderm forms the lens placode (lp) that further invaginates together with the OV to form the optic cup with a lens sphere surrounded by the retina. **(b)** Optical sections through wild-type medaka embryos at indicated stages stained with the antibody against Prox1, a lens placode-specific marker and LFC, a lens fiber cell marker. **(c)** Optical sections through organoids derived from the *Rx3::H2B-GFP* reporter line stained with antibody against Prox1 (magenta) and LFC (cyan). **(d)** Lens specific GFP expression in embryos of the *Foxe3::GFP* reporter line (magenta). Bright-field and GFP fluorescence images showing reporter expression in presumptive lens ectoderm (ple) of day 1 (S19), lens placode (pl) of 1 dpf (S21) and lens (le) of 2 dpf (S24) medaka embryos. **(e)** Optical section through a day 1 organoid (26 hpa) derived from *Foxe3::GFP* reporter line showing the lens-specific expression of GFP (magenta) detected by anti-GFP antibody, co-stained with DAPI (blue). **(f)** Optical section through a day 2 organoid derived from 50 % *Foxe3::GFP* and 50 % *Rx2::H2B-RFP* reporter blastula cells. Expression of RFP (green) and GFP (magenta), detected by antibodies is mutually exclusive, co-stained with DAPI (blue). **(g)** 3D rendering of *Rx2::H2B-RFP* (green), *Foxe3::GFP* (magenta) organoid shown in f, DAPI stained nuclei are in cyan. n numbers in c and e indicate the number of analyzed organoids with described phenotype. LFC, lens fiber cell; le, lens; re, retina; lp, lens placode; SE, surface ectoderm; OV, optic vesicle; dpf, day post fertilization; hpa, hours post aggregation. Dashed line in c, e and f indicates the outline of the organoid. Dashed line in d indicates the outline of the retina. Scale bar 100 µm.

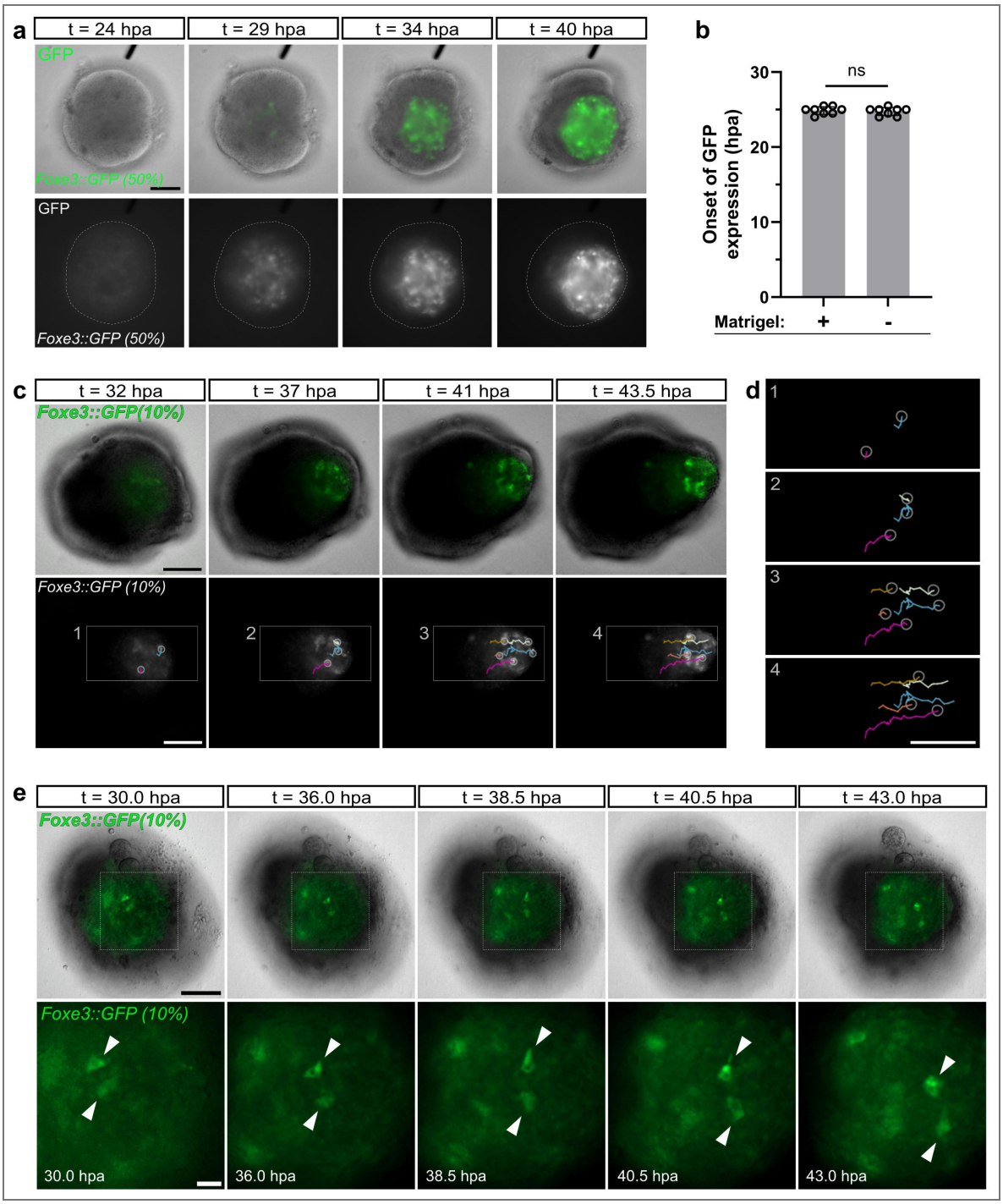

Figure 4. Dynamics of lens formation in ocular organoids.

(a) Single organoid (from Video S2) generated from *Foxe3::GFP* reporter (50 %) and wild-type blastula cells imaged from day 1 (24 h post aggregation; hpa) to day 2 (40 h post aggregation; hpa). Overlay (top panel) of bright-field and GFP fluorescence and GFP fluorescence (bottom panel, gray) of indicated timepoints between day 1 and day 2 organoid development. Dashed lines indicate the outline of the organoid. Total number of n=62 organoids in 4 independent experiments were followed. **(b)** Onset of GFP expression in *Foxe3::GFP*-derived organoids grown with or without Matrigel supplementation at day 1, n=8 organoids per condition. Statistical significance was calculated using an unpaired two-tailed t-test. n.s., not significant. **(c)** Tracking of individual GFP$^+$ cells in the organoids derived from mixture of *Foxe3::GFP* (10 %) and wild-type (90 %) cells from day 1 to day 2. Time indicated in hours post aggregation (hpa). **(d)** Tracks of individual cells over time from details 1-4 in c. **(e)** Movement-associated cell shape changes of GFP$^+$ cells in in the organoids derived from mixture of *Foxe3::GFP* (10 %) and wild-type (90 %) cells from day 1 to day 2. Scale bar 100 µm; enlargement in e: scale bar 25 µm.

and f, arrows). However, at day 4, organoid lenses did not show any apparent lens epithelium (Prox1$^-$/LFC$^-$) (Figure 2g and 2h). In fact, we did not detect any Prox1$^-$/LFC$^-$ cells on the surface of the day 4 lenses, indicating that in organoid lenses a lens epithelium is absent at later stages.

Dynamics of lens formation

Analysis of the cellular composition of day 1 and day 2 organoids showed a stereotypic arrangement of cell types: retinal-committed progenitors established in the epithelialized surface while cells localized in the core of the organoid adopted lens fate and formed centrally localized lens spheres (Figure 3-figure supplement 1d, Figure 3c and 3e). Many morphogenetic events such as germ layer segregation, boundary sharpening, and compartmentalization can be at least partly explained by cell sorting driven by adhesive and mechanical differences (Amack and Manning, 2012; Krieg et al., 2008; Steinberg, 1963; Zhang et al., 2011). To address whether differential adhesive properties of lens and retinal progenitor cells contribute to such cellular arrangements, particularly to the arrangement of lens-committed progenitors into a lens sphere, we performed dissociation/re-aggregation experiment (Figure 4-figure supplement 1a). Day 1 organoids originating from the *Foxe3::GFP* reporter line were dissociated into a single cell suspension to disrupt presumptive retinal/lens domains and to ensure a random distribution of lens-/retina-committed cells (Figure 4-figure supplement 1b-c). Those suspensions were subsequently allowed to re-aggregate (Figure 4-figure supplement 1d, Video S5). Time-laps imaging showed a gradual sorting of *Foxe3::GFP* labeled cells – from single GFP$^+$ cells (Figure 4-figure supplement 1c) through groups of GFP$^+$ cells (after 3h, Figure 4-figure supplement 1d, Video S5) to one single lens localized in the center of the organoid by day 2 (15 h), surrounded by retinal neuroepithelium (AcTub$^+$ cells) (Figure 4-figure supplement 1d and e), scenario resembling organoid organization before dissociation. This data show that differential adhesive properties of lens/retinal precursor cells can enable formation of a compact spherical lens in the center of the organoid.

Although lens progenitors were initially established in the center of the day 1 organoid, the analysis of day 2 and day 4 organoids indicated that the lens was displaced from this initial position to reach the periphery of the organoid by day 2 (Figure 3g, Video S4 and Figure 2b). This was confirmed by time-lapse imaging of ocular organoid development from day 1 to day 2 where *Foxe3::GFP*-expressing cells appear initially in the core region of the organoid at 25 hours post aggregation where they organize into a spherical lens within 16 hours (Video S2, Figure 4a and 4b). This process was accompanied by a gradual shift of the forming lens from center to the periphery where the lens is eventually reaching the surface of the organoid (Video S2, Figure 3f and 3g, Figure 4a). Tracking of individual lens-committed cells supported this trend. Individual centrally located cells collectively moved to the organoid periphery (Figure 4c and 4e, Video S6). This process was accompanied by profound changes in cell shape of tracked *Foxe3::GFP* cells (Figure 4d, Video S7) indicating an active movement of lens progenitors to the organoid periphery. On the other hand, nuclei of retinal cells (*Rx3::H2B-GFP*) followed over same period of time, demonstrated short oscillating movements confined to the retinal neuroepithelium on the surface of the organoid (Video S8), representing interkinetic nuclear migration found in differentiating retinal progenitor cells within the retina. Taken together, these data indicate that differential adhesion-based cell sorting between lens and retinal progenitors together with an active movement of lens progenitor cells from the center to the periphery of the organoid are the driving force of the lens sphere formation and its displacement through the static retinal epithelium.

Lens size scales with organoid size

Since retinal and lens progenitors occupied distinct regions within the organoid, we next investigated how their distribution is affected by total organoid size. We generated organoids from different numbers of cells at day 0 (4,000, 2,000, 1,000 and 500 cells). This approach resulted in organoids of different sizes at day 1: organoids derived from 4,000 cells had an average diameter of 521 ± 13 µm, those from 2,000 cells measured 379 ± 15 µm, from 1,000 cells 310 ± 22 µm, and

from 500 cells 201 ± 55 µm (Figure 5a, 5b and 5d). Interestingly, the thickness of the tissue acquiring retinal progenitor cell identity in the cortex of the ocular organoid (*Rx3::H2B-GFP*) remained constant, independent of the initial size of the aggregate reaching to the depth of: 59.7 µm ± 1.6 µm for 4,000 cells; 55.6 ± 3.1 µm for 2,000 cells; 56.4 µm ± 3.2 µm for 1,000 cells and 55.4 µm ± 6.8 µm for 500 cells (Figure 5b and 5e). While the thickness of retinal neuroepithelium stayed constant, the lens size scaled proportionally with the size of the organoid. By day 4, larger organoids developed larger lenses, whereas smaller organoids formed smaller lenses (224 µm ± 12 µm for 4,000 cells; 199 µm ± 26 µm for 2,000 cells; 115 µm ± 33 µm for 1,000 cells and 68 µm ± 20 µm for 500 cells) (Figure 5c and 5f). Although 500 cell derived organoids were able to form lenses, the efficiency of lens formation was considerably lower (33.3 %; Figure 5g) than in organoids of the bigger sizes (between 86.7 - 95 % for organoids generated by 1,000 or more cells) (Figure 5g). Ocular organoids generated by the aggregation of less than 500 cells did not form any lenses (Figure 5g). Taken together, these data indicate that lens size scales with the size of the organoid and is defined by the constant thickness of the forming retina.

Lens formation depends on temporal activity of FGF and BMP signaling

The competence to form a lens is established during the formation of the anterior neural plate within the region of the anterior neural plate border and is regulated by the coordinated activity of BMP and FGF signaling (Gunhaga, 2011; Litsiou et al., 2005; Sjödal et al., 2007). Once lens competence is established within the SE, FGF and BMP signaling induce its differentiation into the lens placode and subsequently into the lens, accompanied by the expression of structural lens proteins (Faber et al., 2001; Furuta and Hogan, 1998; Le and Musil, 2001; Rajagopal et al., 2009; Sjödal et al., 2007; Wawersik et al., 1999; Zhao et al., 2008). Both BMP and FGF signaling pathways were found to be activated in lens-forming organoids. We used specific antibodies to detect the phosphorylated form of SMAD1/5/8 (pSMAD1/5/8) and ERK kinase (pERK1/2) as downstream effectors of BMP and FGF signaling, respectively (Figure 6a and 6b). BMP signaling activity was detected in the center (region of establishment of lens-committed progenitors (Figure 3e)) of the organoid at day 1 (Figure 6a). On the other hand, only sparse FGF signaling activity (as visualized by pERK1/2) was detected in day 1 organoids, with activity peaking later - at day 1.5 in the center of the organoid. At day 2, FGF activity was observed in both, retinal and lens cells corresponding to the FGF activity in the developing embryo (retina and lens epithelium) at corresponding stage (Figure 6b). To address the contribution of the observed BMP and FGF signaling activity to organoid lens formation, we exposed developing organoids to FGF and BMP antagonists, SU5402 and Noggin or Dorsomorphin, respectively. To separate the establishment of lens competence from the process of lens differentiation, we divided the treatments into two discrete time windows: day 0 to day 1 corresponding to the time before the lens placode formation (establishment of lens competence), and day 1 to day 2 covering lens placode formation and differentiation of lens fiber cells (Figure 6c). We then assessed the organoids at day 2 for the expression of the early lens progenitor marker *Foxe3::GFP* and the differentiation marker LFC.

Blocking BMP signaling with Noggin or Dorsomorphin completely prevented the expression of lens-specific markers if applied from day 0 to day 1 (Figure 6d and 6e) but did not impact on lens formation if administered from day 1 to day 2 (Figure 6d and 6f). In contrast, inhibition of FGF signaling with SU5402-mediated did not affect initial lens formation if applied from day 0 to day 1 and allowed expression of both, lens placode and lens differentiation markers. However, it efficiently blocked the differentiation of lens fiber cells when applied from day 1 to day 2, and completely prevented the expression of the LFC marker (Figure 6d, 6e and 6f). This indicates that similar to embryonic development, the establishment of lens competence (in the center of the organoid between day 0 and day 1) depends on the activity of BMP signaling, while FGF signaling is required later for the lens differentiation process (day 1 to day 2).

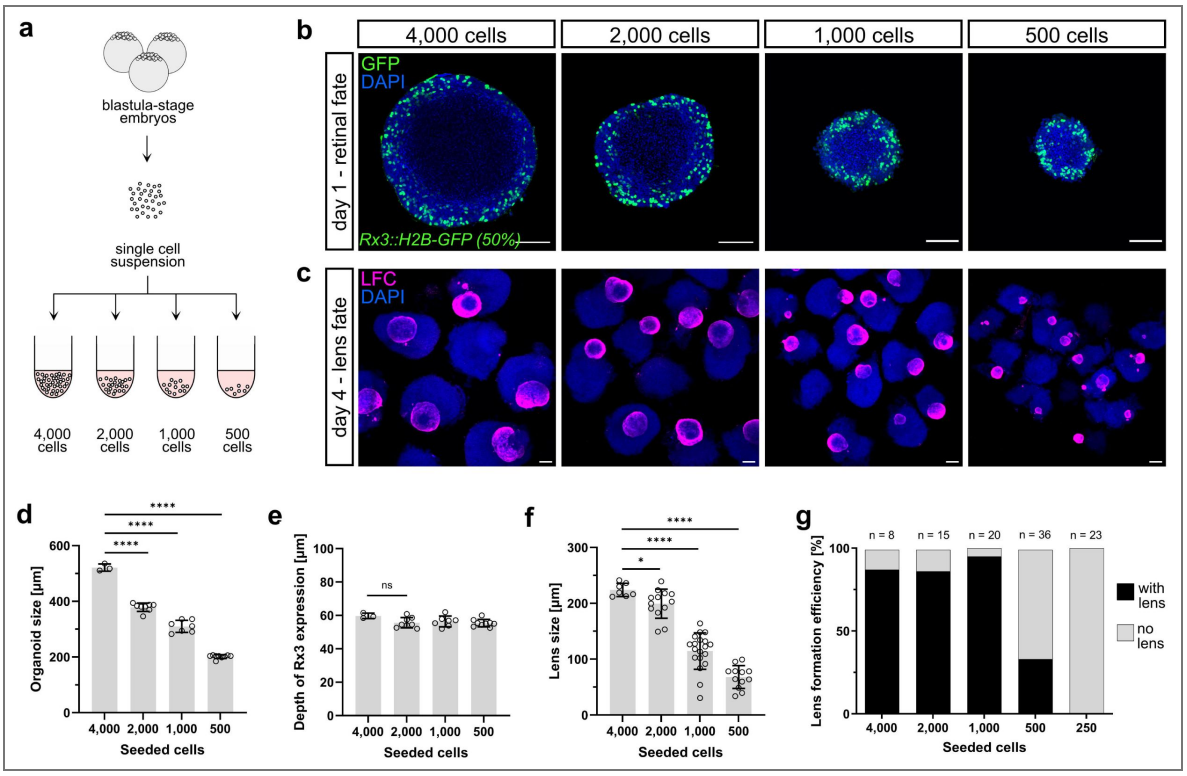

Figure 5. Lens size scales with organoid size.

(a) Schematic representation of generation of organoids of different sizes. Pluripotent embryonic cells were seeded in different seeding densities. **(b)** Representative optical sections of day 1 organoids generated by aggregation of indicated number of cells from *Rx3::H2B-GFP* reporter line immunolabeled with anti-GFP antibody, co-stained with DAPI. For *Rx3::H2B-GFP*, the percentage (%) indicates how many cells carry the indicated transgene. **(c)** Representative images of day 4 organoids generated by indicated number of cells stained with an anti-LFC antibody (maximal z-projections). **(d)** Quantification of diameter of day 1 organoids generated by aggregation of indicated number of cells. **(e)** Quantification of depth of retina-specific marker expression (*Rx3::H2B-GFP*) at day 1 generated by aggregation of indicated number of cells. Number of analyzed organoids: n=3 for 4,000 cells, n=8 for 2,000 cells, n=7 for 1,000 cells, n=9 for 500 cells. **(f)** Quantification of lens size measured as diameter of the lens in day 4 organoids. n=7 for 4,000 cells, n=13 for 2,000 cells, n=19 for 1,000 cells, n=19 for 500 cells. **(g)** Efficiency of lens formation in organoids of different sizes measured as proportion of organoids carrying lens judged by immunolabeling with anti-LFC antibody. Statistical significance was calculated using an unpaired two-tailed t-test. n.s., not significant; ****p<0.0001, *p<0.05. le, lens; re, retina; LFC, lens fiber cell. Scale bar 100 µm.

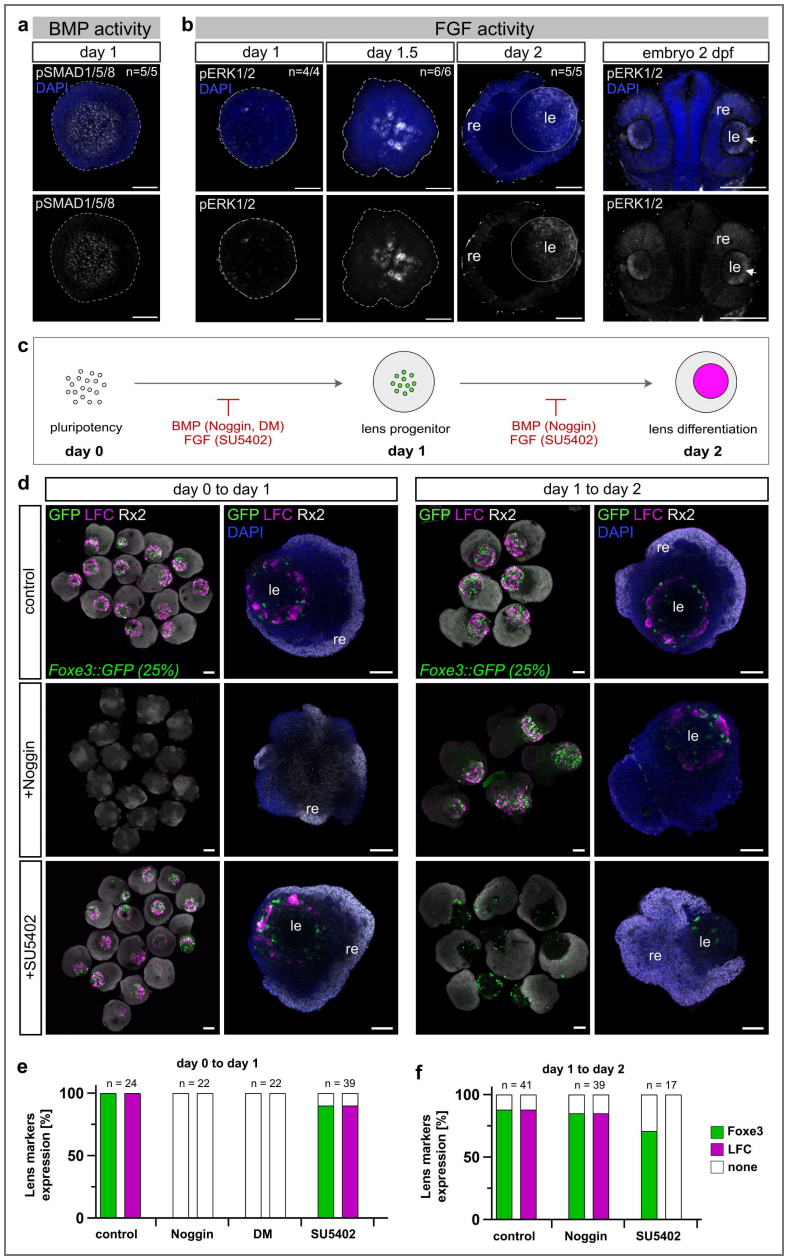

Figure 6. Lens formation is dependent on temporal activity of FGF and BMP signaling.

(a) Activity of BMP signaling detected by immunohistochemistry against phosphorylated SMAD1/5/8 (pSMAD1/5/8) in day 1 organoids. **(b)** Activity of FGF signaling detected by immunohistochemistry against phosphorylated ERK1/2 (pERK1/2) at indicated stages of organoid development and in embryo at 2 dpf. Dashed line indicates the outline of the organoid in day 1 and day 1,5 organoid. In day 2 organoid, line outlines the lens. n numbers indicate the number of organoids with displayed phenotype within one experiment. **(c)** Schematic representation of organoid treatment with FGF and BMP signaling antagonists. Organoids were generated from *Foxe3::GFP* reporter line. Inhibitors of BMP (Noggin, 100 ng/µl or Dorsomorphin -DM, 100 ng/ml) or FGF (SU5402, 10 µM) signaling were administered in time window from day 0 to day 1 or from day 1 to day 2. Organoids were analyzed at day 2 for the expression of lens progenitor marker *Foxe3::GFP* and lens fiber cell differentiation marker LFC. **(d)** Representative images of day 2 organoids treated as indicated and labeled with antibodies against GFP (green), LFC (magenta) and Rx2 (grey). Overview images are represented by maximal z-projections; single organoids are represented by single optical sections. For *Foxe3::GFP*, the percentage (%) indicates how many cells carry the indicated transgene. **(e-f)** Quantification of expression of *Foxe3::GFP* and LFC in control and treated organoids measured as proportion of organoids expressing lens progenitor marker *Foxe3::GFP* (green) and lens differentiation marker LCF (magenta). Total number of n=204 organoids grouped in control and treated groups were analyzed. All treatments were performed in two biological replicates. re, retina; le, lens; DM, Dorsomorphin; LFC, lens fiber cell. Scale bar 100 µm.

Lens organoid gene expression recapitulates the onset of lens-specific genes *in vivo*

To address the temporal dynamics of lens-specific gene expression in *in vivo* and in organoid-based lens development, we performed total RNA sequencing analysis. Embryos at 1, 2, 3, and 4 dpf as well as organoids at corresponding developmental stages, were analyzed for the expression of key markers of lens development. For total RNA sequencing we extracted RNA from whole organoids (composed of both lens and retina), the anterior part of day 1 and 2 embryos (dissected right behind optic vesicles or optic cups), and the eyes of 3 dpf and 4 dpf embryos (Figure 7a). Within the total RNA reads we focused specifically on key genes implicated in the different stages of lens development. Among the genes analysed, the earliest expressed was the transcription factor *Foxe3*, with expression peaking at day 1 of development, followed by the upregulation of the transcription factor *Pitx3* (Figure 7c, Data S1). Day 2 marks the onset of expression of main structural lens proteins in embryos and organoids, namely: crystallins: *cryaa* (αA-crystallin), *cryba1a* (βA1-crystallin), *crybb1l2* (βB1 like 2), *crybb1l3* (βB1 like 3), *cryba2b* (βA2), *cryba4* (βA4), *crybb1* (βB1), *crygn2* (γN2-crystallins), *crygmx* (γMX), *crygm3* (γM3); major lens membrane structural proteins (MIPs/acquaporins) *mipa* and *mipb* coding for water channels ensuring water transport between lens cells (Agre and Kozono, 2003; Donaldson et al., 2024; Varadaraj et al., 1999); Gap junction proteins *Gja8* (connexin-50) and *Gje1* (connexin-23) and lens intrinsic membrane proteins *lim2.2* and *lim2.4* facilitating intercellular transport of metabolites and ions in lens fiber cells (Mathias et al., 2010). Day 3 was characterized by the onset of expression *hsf4* (heat shock transcription factor 4), coding for a transcription factor required for de-nucleation and organelle degradation during lens terminal differentiation (Cui et al., 2013; Gao et al., 2017). Accordingly, *dnase1l1l* (deoxyribonuclease I-like 1-like) and *plaat1* (phospholipase A/acyltransferase) implicated in DNA and lens organelle degradation, respectively (Morishita et al., 2021; Zhang et al., 2020) were also expressed from day 3 of development. At the same stage, the expression of proteins making up the structural scaffold critical for fiber cell architecture and mechanical properties of the lens was initiated. Those include beaded filament proteins *Bfsp1* (filensin) and *Bfsp2* (phakinin) and *Lgsn* (lengsin) (Harding et al., 2008; Perng et al., 2007; Song et al., 2009).

Our comparative analysis indicates highly reminiscent gene expression patterns of key marker genes when comparing organoid and embryonic lens development (Figure 7c, Data S1). This demonstrates that our conditions promote the development of ocular organoids in which the expression of key markers genes is temporally recapitulating the order of expression in the development of the embryonic lens.

Discussion

In vitro organoid development builds on the remarkable ability of embryonic stem cells or progenitor cells to autonomously self-organize in higher order structures with sophisticated microarchitecture, often closely resembling cell type compositions, 3D structure, and the function of the organ (Camp et al., 2015; Dye et al., 2015; Eiraku et al., 2011; Lancaster et al., 2013; McCracken et al., 2014; Nakano et al., 2012).

Here, we used medaka derived pluripotent cells as a model for the generation of complex ocular organoids composed of both, retina and lens. We showed that fish retinal organoids efficiently form embedded lenses, in a process that employs the molecular pathways including expression of key transcription factors and utilization of extracellular signaling pathways, as the embryo. In contrast to *in vivo* development, organoid cells did not follow the canonical process of lens formation, but used an alternative mode of cellular assembly to generate and grow the lens. While in the embryo, the lens sphere is shaped by the coordinated invagination of lens committed head surface ectoderm and retina-forming optic vesicle neuroepithelium, lens progenitors in the organoid were established in a different fashion directly inside of the retinal organoid to form the lens.

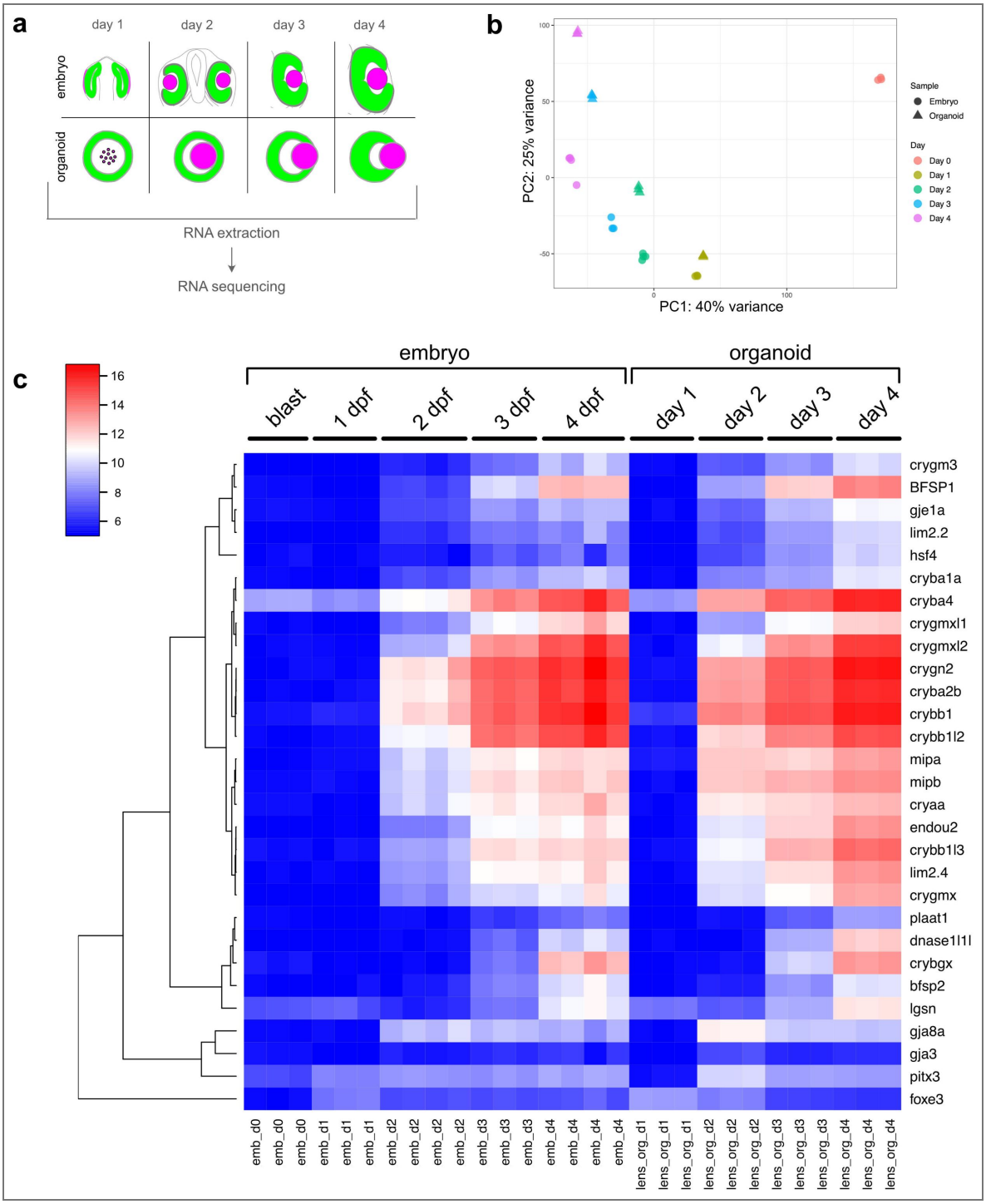

Figure 7. Lens organoid gene expression recapitulates gene expression *in vivo*.

(a) Schematic representation of sample preparation. Whole organoids (composed of both lens and retinal tissue) were analyzed. For 3 dpf and 4 dpf medaka embryos, eyes were dissected (composed of both lens and retina). For 1 dpf and 2 dpf embryos the anterior part of the head right behind optic vesicles or optic cup, respectively was dissected and used for RNA isolation. **(b)** Principal component analysis of the transcriptomes of embryonic and organoid samples at the indicated stages. **(c)** Heatmap clustering of variance stabilized counts of lens-specific genes. Samples were processed in 3 technical replicates each. blast, blastula-stage embryo; emb, embryo; lens_org, lens organoid.

By following early progenitors of both retina (*Rx3*) and lens (*Foxe3*) we found that retina progenitor identity was acquired at the surface, while a spherical domain with lens progenitor identity was established in the center of the organoid (Figure 3c and Figure 3e). While in the embryo the lens originates from the head surface ectoderm, non-canonical routes to lens regeneration have been described in some species. In newts, the lens can be regenerated from the pigmented epithelial cells of the iris after injury or lens removal (Agata et al., 1993; Grogg et al., 2005; Maki et al., 2007). Lens formation was also observed in the cultures of chick neuroretinal cells (Iida et al., 2017; Okada et al., 1975) showing that retinal-fated cells can give rise to lens cells under certain circumstances. However, in medaka ocular organoids, retina and lens are formed by spatially separated populations of retina- and lens-committed progenitor cells.

The size of the lens scaled with the size of the organoid and was limited by the volume of the organoid that acquired retinal fate (Figure 5). The constant depth of retinal fated cells in the cortex under the surface of the organoid, regardless of the size of the aggregate, suggests that retinal fate is influenced by environmental gradients, which cause the diffusion-limited availability of retina-inducing factors. It has previously been shown that cells on the surface of the organoid experience higher level of oxygen tension, higher level of nutrients and signaling molecules than cells located more centrally (Grün et al., 2023; McMurtrey, 2016; Qian et al., 2019; Tse et al., 2021) when grown in 3D suspension culture. Additionally, cells at the surface experience different mechanical forces, mostly due to the interactions with ECM (Vining and Mooney, 2017). Both, retinal as well as lens fates, were established either before ECM addition or in the absence of Matrigel (Zilova et al., 2021, this study), making the environmental gradient more likely to contribute to the observed tissue arrangement in fish organoids.

Interestingly, Bmp inhibition in the early stages of organoid development, before the appearance of *Foxe3*-expressing lens progenitor cells (day 0 to day 1) completely abolished lens formation, while BMP inhibition during the lens formation process (from day 1 to day 2) did not show any impact. Thus, we hypothesize that a source of BMP in the forming neuroretina establishes initial lens competence in the center of the organoid. During normal development, BMP4 is secreted by the neuroepithelium of the developing OV and was found to be essential for lens induction (Furuta and Hogan, 1998; Rajagopal et al., 2009). Accordingly, ablation of the prospective neuroectoderm in chick (Kamachi et al., 1998) or defective OV formation in mouse (Klimova and Kozmik, 2014; Mathers et al., 1997; Porter et al., 1997) prevents lens formation, indicating that the developing neuroepithelium stimulates lens formation within the pre-placodal ectoderm. The emergence of lens fate in the center of ocular organoids consequently depends on a critical threshold of the morphogen to be reached in the center. The scaling of lens size with organoid size supports this hypothesis as larger organoids are better suited to reach this threshold - potentially due to increased total ligand production (in the forming neuroretina) resulting in the formation of a more pronounced gradient.

During normal development, developing retinal cells have been suggested to serve as a source of FGFs stimulating expression of lens structural genes and inducing lens differentiation (Chow et al., 1995; Faber et al., 2001; Gunhaga, 2011; Le and Musil, 2001; McAvoy et al., 1999; Robinson, 2006; Zhao et al., 2008). Accordingly, blocking of FGF signaling activity during organoid lens formation prevented lens differentiation. The dependency of lens formation on the activity of BMP and FGF signaling pathways has been well documented also in other *in vitro* systems where transient activation of BMP and FGF signaling is necessary for the *in vitro* differentiation of lens-like structures (lentoid bodies) (Dincer et al., 2013; Fu et al., 2017; Leung et al., 2013; Yang et al., 2010).

Since organoids show remarkable similarities to their *in vivo* counterparts when it comes to cellular composition and key structural features, we naturally tend to infer that corresponding structures are formed by corresponding cellular processes in both systems. Here we show an example of an alternative mode of cellular assembly that leads to a similar structural and molecular outcome. In the embryo, the lens formation is driven by invagination of the lens placode to generate a lens pit and finally a spherical lens. In organoids on the other hand, individual lens-committed progenitors are established in the center of the organoid. Our current

data support the hypothesis, that differential adhesive properties of lens and retinal progenitor cells mediated by preferential homotypic cell-cell adhesion support the formation of the lens sphere. Concomitant active movement of lens-committed progenitors from the organoid center to its periphery through the retinal sheet on the surface places the lens to the superficial position, resulting in the observed optic cup-like morphology of the organoid. Our observation that dissociated organoid cells re-aggregate into homotypic clusters is consistent with classical and more recent work showing that differential adhesion, often combined with differential contractility, can drive robust cell sorting in both embryonic tissues and *in vitro* systems. Such adhesion-based sorting is now regarded as a generic mechanism that frequently contributes to tissue assembly and compartmentalization during embryonic development, alongside complementary processes such as active cell migration and contact inhibition of locomotion (Amack and Manning, 2012; Brayford et al., 2019; Davis et al., 2012; Krieg et al., 2008; Zhang et al., 2011).

Organoids can recapitulate many aspects of embryonic development. However, the absence of embryonic constraints can also lead to significant differences in tissue organization, cellular interactions, and overall structure. While the goal of many organoid studies is to replicate *in vivo* conditions as closely as possible (Chen et al., 2024; Hofer and Lutolf, 2021; Kretzschmar and Clevers, 2016; Sahu and Sharan, 2020; Zhao et al., 2022), the unconstrained environment of organoids offers a unique opportunity to tap the organoid's potential of self-organization. This can uncover alternative developmental pathways that are not apparent *in vivo* and could expand our understanding of the plasticity, robustness and adaptability of developmental programs when unleashed from evolutionary constraints. Insights gained from alternative assembly processes could inform the design of synthetic biological systems and potentially lead to innovative strategies for creating complex tissues and organs *in vitro*.

Materials and Methods

Fish handling and maintenance

Medaka (*O. latipes*) stocks were maintained according to the local animal welfare standards (Tierschutzgesetz §11, Abs. 1, Nr. 1, husbandry permit AZ35-9185.64/BH, line generation permit number 35–9185.81/G-145/15 Wittbrodt). The following medaka lines were used in this study: Cab strain as a wild type (Loosli et al., 2000), *Rx3::H2B-GFP* (Rembold et al., 2006), Rx2::H2B-GFP (Inoue and Wittbrodt, 2011), *Atoh7::EGFP* (Del Bene et al., 2007), *Gaudí*^{RSG} (Centanin et al., 2014), *Foxe3::GFP* (this study).

Generation of organoids

Organoids were generated as previously described (Zilova et al., 2021) with slight modification of the protocol. Blastula stage embryos, stage 11 (Iwamatsu, 2004) were de-chorioneated, cells mass was isolated and washed twice with PBS (Thermo Fisher Scientific, Cat#:10010023). Cell mass was dissociated in PBS by pipetting up and down and centrifuged through 40 µm strainer (pluriSelect, Cat#:43-10040-51) for 3 min at 180 x *g*. Pellet was re-suspended in differentiation media: DMEM/F12 (Gibco, Cat#:11320033), 5 % KSR (Gibco, Cat#:10828028), 1x NEAA (Sigma-Aldrich, Cat#:M7145), 1x sodium pyruvate (Sigma-Aldrich, Cat#:S8636), 1x penicillin/streptomycin, 20 mM Hepes pH 7.4 (Roth, Cat#:9105.4), 0.1 µM Φ3-mercaptoethanol (Gibco, Cat#:21985-023). If not stated otherwise, 3.000 cells per aggregate in 100 µl were seeded into individual wells of low-binding 96-well plate (Thermo, Cat#:174925 Nunclon Sphera). Cells were incubated in 26°C in the incubator without CO_2 control. At day 1, aggregates were washed in differentiation media, Matrigel (Corning, Cat#:356238) was added to final concentration of 2 % and aggregates were incubated in humidified tissue culture incubator under 5 % CO_2 condition.

To label specific population of cells, organoids were generated from fish reporter lines expressing fluorescent protein under the control of tissue specific promotor/enhancer (*Cry::ECFP*; *Rx3::H2B-GFP*; *Rx2::H2B-RFP*; *Atoh7::EGFP*; *FoxE3::GFP*). In that case, cells were extracted from the blastula stage embryos originating from the outcross of fish reporter line and wild-type fish, and in some

cases further mixed with cells originating from wild-type embryos of the same stage to achieve sparse labeling. The proportion of cells coming for transgenic reporter line genetically able to express the transgene is indicated in the figures in percentage (%).

Treatment of cells/aggregates/organoids

Cells or aggregates were treated with Noggin (Merck Millipore, Cat#:GF173, 100 ng/ml), Dorsomorphin (Merck, Cat#:171260, 100 ng/ml), or SU5402 (Sigma, Cat#:SML0443, 10 µM). For treatment from day 0 to day 1, blastula stage cells were resuspended directly in differentiation media containing an antagonist in desired concentration. At day 1 (16 hours post aggregation), aggregates were washed twice with fresh differentiation media, supplemented with 2% Matrigel (Corning, Cat#:356238) in differentiation media and incubated till day 2. For treatment from day 1 to day 2, day 1 aggregates (16 hours post aggregation) were washed with differentiation media and transferred into antagonist-containing media and immediately supplemented with 2% Matrigel diluted in antagonist-containing media and incubated till day 2. All organoids were fixed at day 2 and analyzed for the presence of lens and retinal tissues by immunohistochemistry.

Dissociation and re-aggregation of organoids

Day 1 organoids (25 hours post aggregation) derived from *Foxe3::GFP* reporter line (100% cells labeled) were washed in PBS (Thermo Fisher Scientific, Cat#:10010023) and dissociated in mixture of Trypsin (2.5 %; Gibco, Cat#:15090-046) and Dispase (1 U/ml; STEMCELL Technologies, Cat#:07923) in ratio 1:1. 5-10 organoids we dissociated in 150 µl of dissociation mix for 10 min at 32°C. Dissociation was stopped by addition of 150 µl of 50 % FBS (Gibco, Cat#:10063732) in PBS. Cell suspension was centrifuged through 40 µm strainer (pluriSelect, Cat#:43-10040-51) for 3 min at 180 x g and pellet was re-suspended in differentiation media: DMEM/F12 (Gibco, Cat#:11320033), 5 % KSR (Gibco, Cat#:10828028), 1x NEAA (Sigma-Aldrich, Cat#:M7145), 1x sodium pyruvate (Sigma-Aldrich, Cat#:S8636), 1x penicillin/streptomycin, 20 mM Hepes pH 7.4 (Roth, Cat#:9105.4), 0.1 µM Φ3-mercaptoethanol (Gibco, Cat#:21985-023) and seeded into wells of low-binding 96-well plate (Thermo, Cat#:174925 Nunclon Sphera). Cells were incubated in 26°C in humidified tissue culture incubator under 5 % CO_2 condition or imaged with ACQUIFER Imaging Machine (ACQUIFER Imaging GmbH, Heidelberg, Germany) (Pandey et al., 2019).

Fluorescent labeling

Fish embryos and organoids were fixed in 4% PFA overnight at 4°C, washed with PTW (PBS supplemented with 0.1 % Tween 20), permeabilized by incubation in acetone for 15 min in - 20°C and washed tree times with PTW. Samples were blocked in PTW supplemented with 4 % sheep sera (Sigma, Cat#:14C509), 1 % BSA (Sigma, Cat#:4503) and 1 % DMSO (Sigma, Cat#:D4540) and incubated with primary antibody diluted in 0.1 x blocking solution overnight at 4°C. Primary antibodies used in this study: rabbit anti-Rx2 (Reinhardt et al., 2015) (1:500), chicken anti-GFP (Invitrogen, Cat#:A10262, 1:500), mouse anti-lens fiber cell (Abcam, Cat#:ab185979, ZL-1, 1:500), rabbit anti-Prox1 (Millipore, Cat#:AB5475, 1:2000), rabbit anti-RFP (Clontech, Cat#:632496, 1:500), rabbit anti-pSMAD1/5/8 (Cell Signaling, Cat#: 9511S, 1:500); rabbit anti-pERK1/2 (Cell Signaling, Cat#:4370, 1:500); mouse anti-acetylated tubulin (Sigma, Cat#: T7451, 1:500). Samples were washed with PTW and incubated with the mixture of DAPI nuclear stain (Sigma, Cat#:D9564, 1:500) and secondary antibodies diluted in 0.1 x blocking solution overnight at 4°C. Secondary antibodies used in this study: donkey anti-mouse 647 (Jackson, Cat#:105869, 1:750), donkey anti-chicken 488 (Jackson, Cat#:703-545-155, 1: 750), donkey anti-rabbit 594 (Invitrogen, Cat#:A21207, 1:750). Samples were washed with PTW. For detection of proliferating cells, Click-iT EdU Alexa Fluor 647 Imaging Kit (Invitrogen, Cat#:C10340) was used according to manufacturer instructions. All immunolabeled samples were transferred into clearing solution composed of: 20% urea (Vetec, Cat#:V900119), 30% D-sorbitol (Vetec, Cat#:V900390), 5% glycerol (Vetec, Cat#:V900122) in DMSO (Vetec, Cat#:V900090) (Zhu et al., 2019) and imaged with laser scanning confocal microscope Sp8 (Leica).

Imaging

Fixed immunolabeled samples were imaged in MatTek glass bottom dish (Mattek, Cat#:D35G-1.5-10-C) with Sp8 confocal microscope (Leica). Organoids overview bright-field pictures were taken with wide-field microscope (Mi8; Leica). For live imaging of lens formation (Video S2, Figure 4a), organoids generated from *Foxe3::GFP* reporter line (50 % of reporter cells mixed with 50 % of wild-type cells) were imaged from day 1 (24 h post aggregation) to day 2 (40 h post aggregation). Imaging was caried out at 26°C directly in low binding 96-well plate (Thermo, Cat#:174925 Nunclon Sphera) with ACQUIFER Imaging Machine (ACQUIFER Imaging GmbH, Heidelberg, Germany) (Pandey et al., 2019). For each well, a set of 10 z-slices (70 µm step size) was acquired in the bright field (50% LED intensity, 40 ms exposure time) and 470 nm fluorescence (50% LED excitation source, FITC channel, 200 ms exposure time) channels. Imaging was performed over 16 hr of organoid development with 30 min intervals. For live imaging of re-aggregation of dissociated cells (Figure 4-figure supplement 1d and Video S5), organoids generated from *Foxe3::GFP* reporter line (100 % of reporter cells) were imaged from day 1 (25 h post aggregation/1 h after dissociation) to day 2 (15 h after dissociation). Imaging was caried out at 26°C directly in low binding 96-well plate (Thermo, Cat#:174925 Nunclon Sphera) with ACQUIFER Imaging Machine (ACQUIFER Imaging GmbH, Heidelberg, Germany) (Pandey et al., 2019). For each well, a set of 30 z-slices (10 µm step size) was acquired in the bright field (50 % LED intensity, 40 ms exposure time) and 470 nm fluorescence (100 % LED excitation source, FITC channel, 50 ms exposure time) channels. Imaging was performed over 15 hr of with 1 h intervals.

For tracking of individual cells (Figure 4c and 4e; Video S6, S7 and S8), organoids generated from *Foxe3::GFP* (10 % of cells from transgene mixed with 90% of cells from wild-type embryos to ensure sparse labeling) or *Rx3::H2B-GFP* (2 % of cells from transgene mixed with 98% of cells from wild-type embryos to ensure sparse labeling) reporter line were imaged from day 1 (30 h post aggregation) to day 2 (43.5 h post aggregation). Imaging was caried out at 26°C directly in low binding 96-well plate (Thermo, Cat#:174925 Nunclon Sphera) with ACQUIFER Imaging Machine (ACQUIFER Imaging GmbH, Heidelberg, Germany) (Pandey et al., 2019). For each well, a set of 30-50 z-slices (9 µm step size) was acquired in the bright field (50% LED intensity, 40 ms exposure time) and 470 nm fluorescence (100 % LED excitation source, FITC channel, 50 ms exposure time) channels. Imaging was performed with 30 min intervals.

Images were processed with Fiji (Schindelin et al., 2012). Cell tracking was performed using Manual tracking with TrackMate plugin in Fiji (Ershov et al., 2022).

Transcriptome analysis

RNA was isolated from 1 dpf, 2 dpf, 3 dpf and 4 dpf medaka embryos as indicated in Figure 7a. Material from 6 embryos per condition was pooled. For embryos 1 and 2 dpf, head region containing optic vesicle and head structure anterior to the optic vesicles and eye cup and tissue anterior to the eye respectively were dissected in ice cold PBS. For stages 3 dpf and 4 dpf, eyes were dissected in ice cold PBS. Considering 3 h delay in organoid development with the respect to embryonic development (Zilova et al., 2021), organoids were collected for RNA isolation 3 h later than the embryonic tissue. For organoids, 20 organoids were pooled per condition. Samples were prepared in three replicates. Samples were rinsed with ice cold PBS and homogenized in 200 µl of Trizole and RNA was isolated using Direct-zol RNA Microprep (Zymoresearch, Cat#:R2060) according to the manufacture protocol. Library preparation was performed with the NEBNext Ultra II RNA Library Prep Kit for Illumina with NEBNext Poly A Selection Kit and NEBNext Multiplex Oligos with UMI. Input RNA was quantified with the Qubit BR RNA assay, and qualified on the Agilent Tapestation (RNA Assay), libraries were quantified with the Qubit DNA HS Assay, and qualified on the Agilent Tapestion (D1000 Assay). Libraries were sequenced on the Illumina NextSeq 550 Sequencer.

For downstream bioinformatic analysis, UMIs were extracted using UMI-Tools v1.1.2 (Smith et al., 2017). The first 12 bases of each read were trimmed, and reads shorter than 50 bases with an average quality lower than 20 were discarded using Trimmomatic v0.39 (Bolger et al., 2014).

Processed reads were mapped to the Japanese medaka HdrR reference genome ASM223467v1 using Bowtie 2 v2.4.4 (Langmead and Salzberg, 2012), and deduplication of the mapped reads was performed with UMI-Tools v1.1.2 (Smith et al., 2017). Gene counts were extracted with featureCounts v2.0.3 (Liao et al., 2014) using the Ensembl version 113 GTF as a reference. The subsequent analysis was performed using R v.4.4.1 (*https://www.r-project.org/*). Genes with fewer than 10 counts across samples were excluded, and DESeq2 (Love et al., 2014) was used for normalization and variance stabilizing transformation of the gene counts. The transformed counts were then used for principal component analysis and heatmap visualization of lens-specific gene expression.

Generation of *FoxE3::GFP* reporter line

1.5 kb region upstream of *Foxe3* (ENSORLG00000017669) ATG was PCR amplified from medaka fish genomic DNA with Q5 High Fidelity DNA Polymerase (NEB, Cat#:M0491) using following primers: KpnI-FoxE3 (forward primer): 5'-TAAGGTACCTGGAATCAAGCAGAAATAATCCACCAAAAGCA and FoxE3_R1 (reverse primer): 5'-GGGGTACCGTTGCACATGCCAGAGAAGTAG, sub-cloned into pJet1.2/blunt cloning vector (Thermo Fisher Scientific), released via restriction digest with XhoI (NEB, Cat#:R0146) and NcoI (NEB, Cat#:R0193) restriction enzymes. The plasmid ISceI-pBSII KS+ (NovoPro, Cat#:V009906) (containing GFP sequence inserted via EcoRI and XbaI restriction sites) was digested with XhoI and NcoI, and ligated with the 1.5 kb *Foxe3* upstream regulatory element to generate *I-Sce/FoxE3(1.5kb)::*GFP. Plasmid DNA was isolated with QuiAprep Spin Miniprep Kit (Quiagen, Cat#:27106), sequenced (Eurofins Genomics) and analyzed using Geneious R8.1 (Biomatters). *I-Sce/FoxE3(1.5kb)::*GFP (10 ng/µl) was co-injected with Meganuclease (I-SceI) (NEB, Cat#:R0694L) into the cytoplasm of one cell stage medaka zygotes as previously described (Thermes et al., 2002) to generate *Foxe3::GFP* reporter line. Embryos were raised and maintained at 26°C in 1× Embryo Rearing Medium (ERM, 17 mM NaCl, 40 mM KCl, 0.27 mM $CaCl_2$, 0.66 mM $MgSO_4$, 17 mM HEPES) and screened for ocular GFP expression 1 dpf on a Nikon SMZ18.

Quantitative analysis of organoid and lens size

Organoid and lens sizes (Figure 2-figure supplement 1, Figure 5d and 5f) were measured as diameter (mean of 4 measurements per organoid) of the organoid on central optical section through organoid (organoid size at day 1) or on maximal projection of multiple z planes of the organoid (lens size at day 2, 4 or 5). Depth of *Rx3::H2B-GFP* expression (Figure 5e) was measured on central optical section through the organoid (mean of 8 measurements per organoid) as a thickness of tissue carrying GFP^+ cells. Statistical analysis and plots were prepared with GraphPad. Figures were assembled with Affinity Designer 2.

Supplementary figures

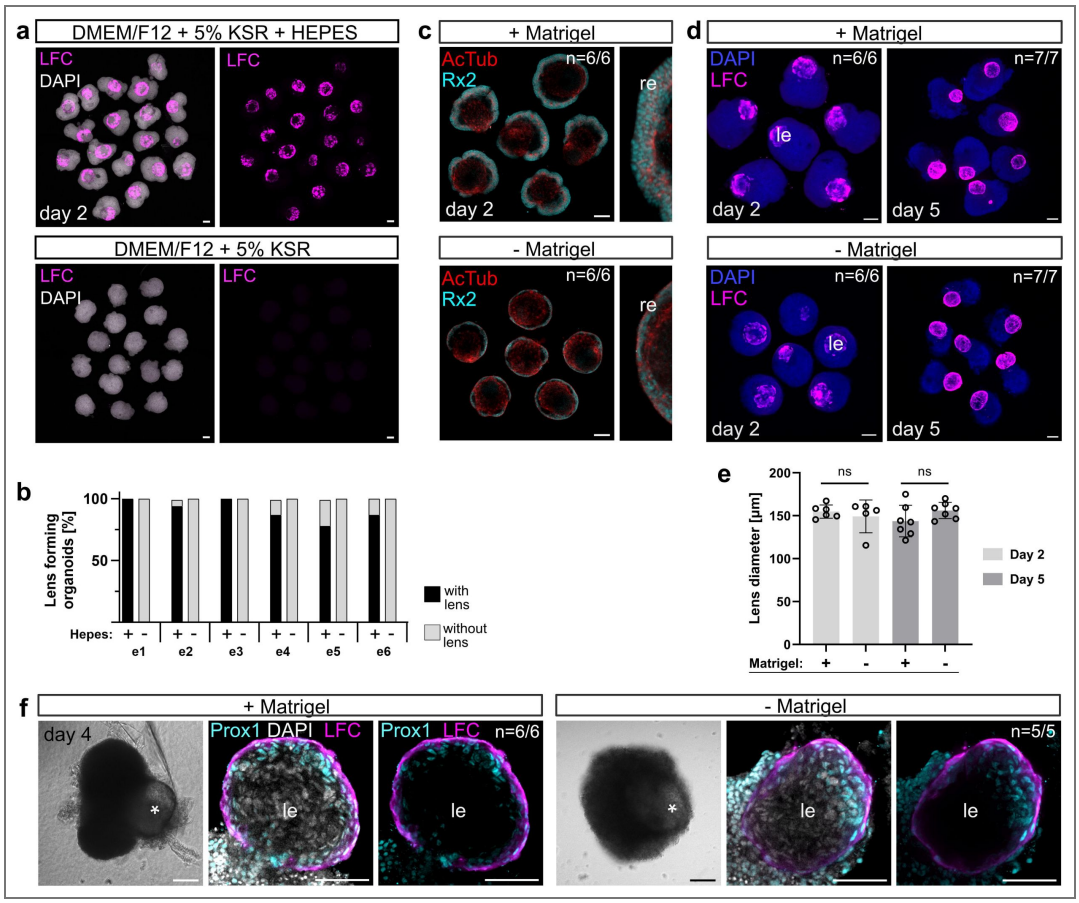

Figure 2-figure supplement 1. Expression of lens-specific markers is dependent on the presence of HEPES in the media and occurs independently of Matrigel addition, related to Figure 1 and Figure 2. (a) Day 2 organoids generated in DMEM/F12 + 5 % KSR media in the presence or absence of 20 mM HEPES labeled with anti-LFC antibody, co-labelled with DAPI nuclear stain. **(b)** Quantification of the efficiency of lens formation measured by the expression of lens marker LFC in day 2 organoids grown in differentiation media with or without HEPES in n=6 independent experiments (e1 – e6). Total number of analyzed organoids: n=63 without HEPES; n=83 with HEPES. **(c-f)** Impact of Matrigel supplementation on organoid organization. **(c)** Day 2 organoids supplemented or not supplemented with Matrigel (2 % final concentration) at day 1 labeled with anti-Rx2 and anti-AcTub (acetylated tubulin) antibody to visualize the structure of retinal neuroepithelium. **(d)** Day 2 and day 5 organoids supplemented or not supplemented with Matrigel (2 % final concentration) at day 1 labeled with anti-LFC antibody (displayed as maximal projections of multiple z planes). **(e)** Quantification of the size of the lens measured as the diameter of LFC^+ lens sphere in d. Statistical significance was calculated using an unpaired two-tailed t-test. n.s., not significant. **(f)** Day 4 organoids labelled with anti-GFP and anti-LFC antibody, co-labeled with DAPI nuclear stain, represented by single optical section. The effect of Matrigel supplementation was assessed in total of n=49 organoids in 4 independent experiments. n numbers indicate the number of organoids with displayed phenotype within one experiment. LFC, lens fiber cell; re, retina; le, lens. Scale bar in a, c, d, and f: 100 µm, in enlarged lens in f: scale bar 50 µm.

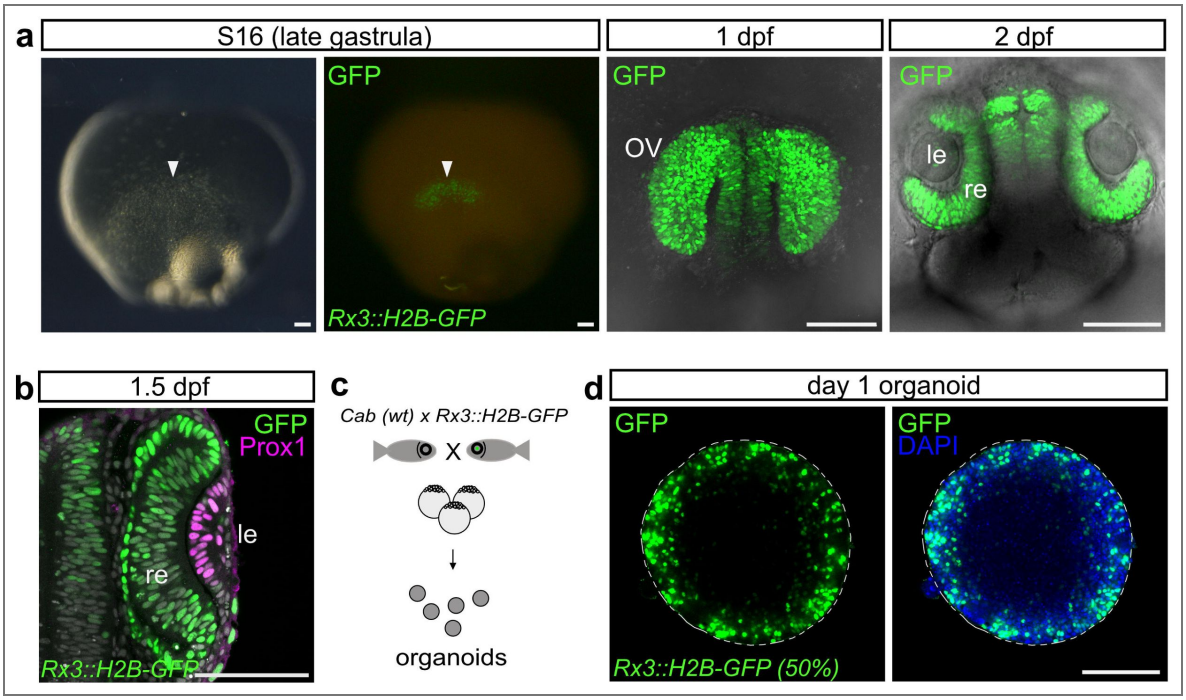

Figure 3-figure supplement 1. Expression domain of *Rx3::H2B-GFP* in the embryo and organoid, related to Figure 3.

(a) Expression domain of *Rx3::H2B-GFP* in medaka fish embryo at indicated stages showing the expression in the anterior neural plate - presumptive eye field (S16, late gastrula stage, arrowhead), retina-committed progenitors of the optic vesicle (1 dpf), retina and forebrain (2 dpf). 1 dpf is represented by maximal z-projection. 2 dpf represented by single optical section through a live embryo. **(b)** Optical section through medaka fish embryo 1.5 dpf (S22) immunostained with antibodies against GFP and Prox1 showing lens-specific expression of Prox1 and retina-specific expression of *Rx3::H2B-GFP*. **(c)** Schematic representation of organoid generation from the retina-specific *Rx3::H2B-GFP* reporter line (50 % of cells). **(d)** Single optical section showing peripheral expression of retina specific marker *Rx3::H2B-GFP* in the organoid at day 1 visualized by immunohistochemistry with antibody against GFP; co-stained with DAPI nuclear stain. For *Rx3::H2B-GFP*, the percentage (%) indicates how many cells carry the indicated transgene. Dashed line indicates the outline of the organoid. wt, wild type; le, lens; re, retina; OV, optic vesicle. Images acquired with laser scanning confocal microscope sp8 (Leica). Scale bar 100 µm.

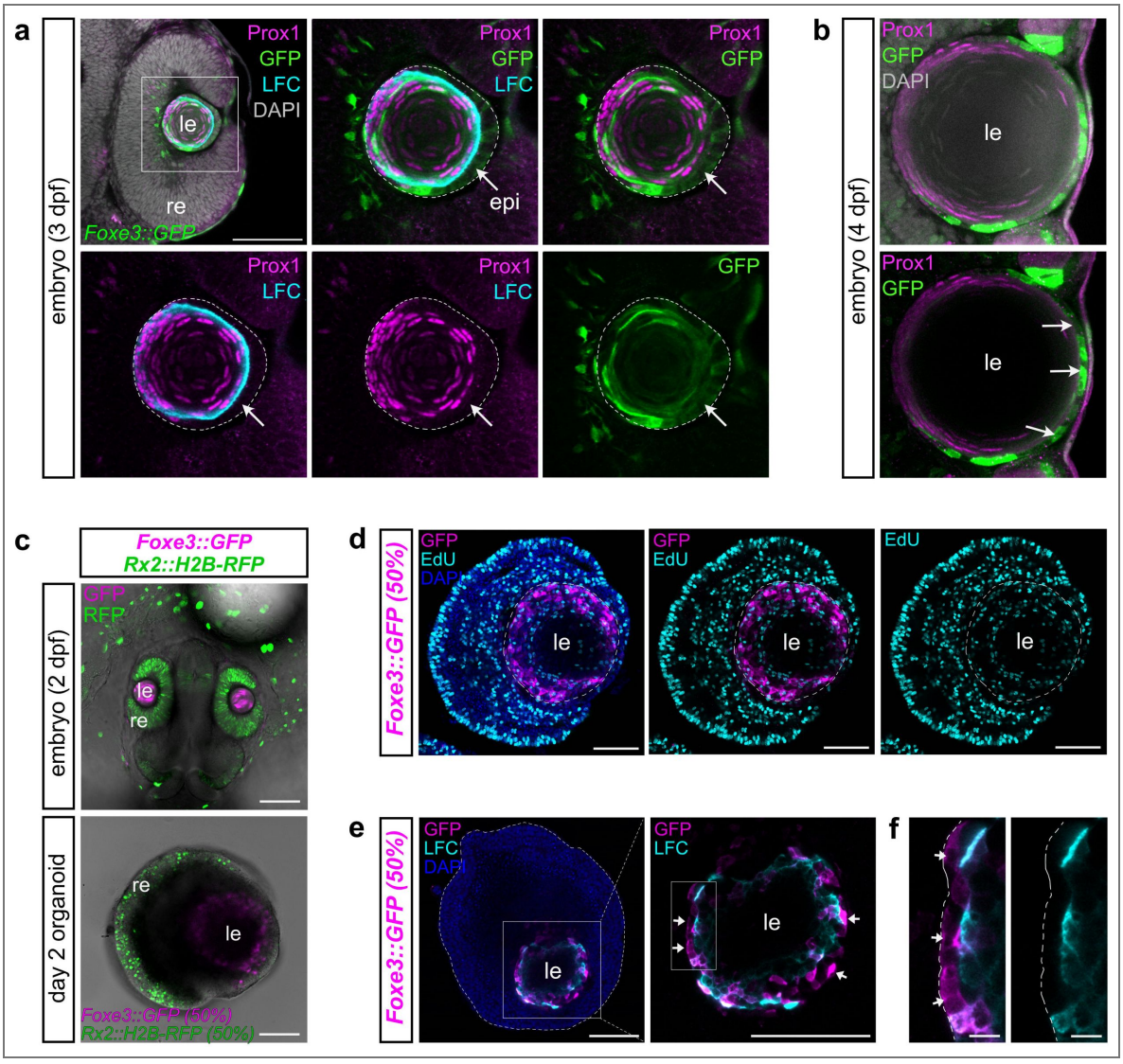

Figure 3-figure supplement 2. Characterization of *Foxe3::GFP* reporter-expressing cells in embryos and organoids, related to Figure 3.

(a-b) Expression of *Foxe3::GFP* in medaka embryonic lens. Optical sections of the whole eye and magnification of lens at 3 days post fertilization (a) and lens at 4 days post fertilization (b) showing the expression of *Foxe3*-driven GFP in lens epithelium (arrows) and differentiating lens fiber cells (core of the lens), co-labeled with the antibody against Prox1 and LFC lens fiber cell antibody. Dashed line indicates the outline of the lens in a. **(c)** Expression of *Rx2::H2B-GFP* and *Foxe3::GFP*, in the day 2 embryo and organoid. **(d)** EdU incorporation assay labeling proliferating (S-phase) cells in day 2 *Foxe3::GFP*-derived organoids exposed to EdU for 1 hour, GFP (magenta) and EdU (cyan) were detected by immunolabeling with anti-GFP antibody and EdU detection. **(e)** Distribution of *Foxe3*-driven GFP and lens differentiation marker LFC. Dashed line indicates the outline of the organoid. **(f)** Detail of indicated area in e highlighting *Foxe3::GFP*$^{+}$/LFC^{-} cells, similar to the progenitor-carrying lens epithelium in embryonic lens (arrows). Dashed line indicates the outline of the lens. For *Foxe3::GFP* and *Rx2::H2B-RFP*, the percentage (%) indicates how many cells carry the indicated transgene. le, lens; re, retina; epi, lens epithelium; LFC, lens fiber cell; dpf, days post fertilization. Scale bar 100 µm.

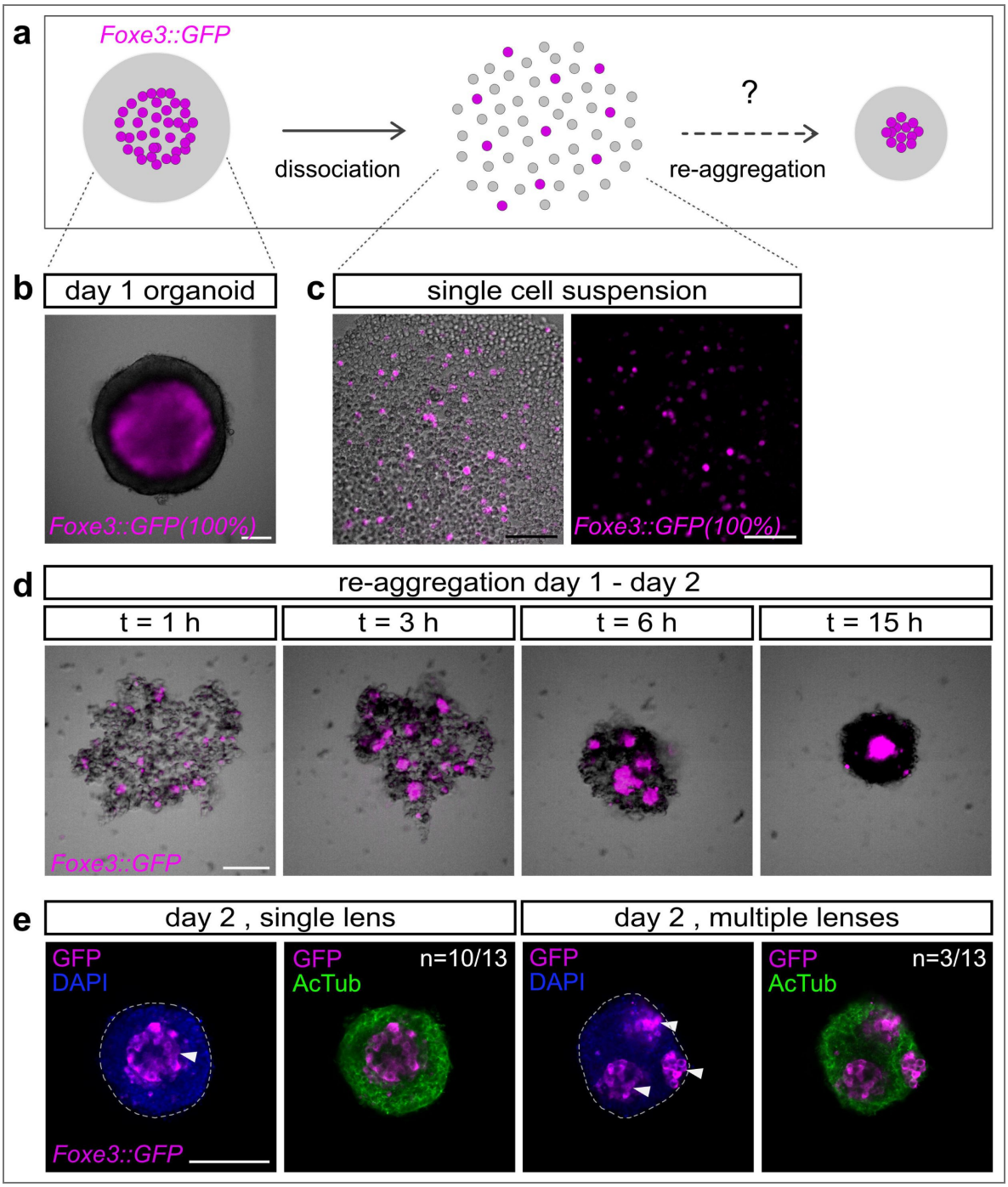

Figure 4-figure supplement 1. Retinal and lens progenitor cells show differential adhesive properties allowing for cell identity-based cell sorting.

(a) Schematic representation of dissociation/re-aggregation experiment. Day 1 organoids derived from *Foxe3::GFP* lens reporter line were dissociated into single-cell suspension and left to re-aggregate. **(b)** Representative picture of day 1 *Foxe3::GFP* organoid before dissociation showing lens-specific GFP expression in the central region of the organoid. (c) Single cell suspension generated by trypsin-mediated organoid dissociation. **(d)** Process of re-aggregation showing gradual sorting of *Foxe3::GFP*-expressing lens progenitors. Time (t) indicated in hours post dissociation. **(e)** Representative images of organoids generated by dissociation/re-aggregation process showing distribution of retinal ($AcTub^+$) and lens (GFP^+) cells analyzed by immunohistochemistry. In 3 independent experiments, total number of n=35 organoids were analyzed. n numbers in e indicate the number of organoids with displayed phenotype within one experiment. Scale bar 100 µm.

Data availability

Source Data files containing numerical data used in figures Figure S1, Figure 4b, Figure 5d-g, Figure 6e and 6f are provided as Excel tables and labelled accordingly. Source Data file: Data S1 provides source data (normalized and variance stabilized counts labeled with Ensemble IDs) used for transcriptome analysis presented in Figure 7. Bulk RNA sequencing data have been deposited in publicly available repository of Heidelberg University, HeiData and are publicly available under *https://doi.org/10.11588/DATA/VEREK9* as of the date of publication. This manuscript does not report original code.

Acknowledgements

The authors thank to E. Hasel de Carvalho and J. Benjaminsen for valuable discussions and comments on the manuscript, T. Kellner and B. Wittbrodt for technical help and maintaining fish stocks. Library preparation and sequencing was performed by CCTP Deep Sequencing Facility of Heidelberg University.

This work was supported by grants of the Excellence Cluster “3D Matter Made to Order” (EXC-2082/1-390761711) funded through the German Excellence Strategy via Deutsche Forschungsgemeinschaft (DFG, German Research Foundation), PostDoc take-off Grant funded through and the Excellence Cluster ‘3D Matter Made to Order’ to L.Z. and J.W and Dr. Moos-Stiftung. For the publication fee, we acknowledge financial support by Heidelberg University.

Additional information

Lead contact

Requests for further information and resources should be directed to the lead contact, Lucie Zilova (*lucie.zilova@cos.uni-heidelberg.de*).

Materials Availability Statement

Plasmids and fish lines generated in this study will be made available on request, but we might require a completed materials transfer agreement if there is potential for commercial application.

Author Contributions Statement

Conceptualization: L.Z., J.W.

Investigation: E.S., M.A.D.T., L.Z., A.P., I.S.

Visualization: E.S., M.A.D.T., I.S., L.Z.

Funding acquisition: J.W., L.Z.

Project administration: J.W. Supervision: L.Z.

Writing - original draft: L.Z., J.W.

Funding

Funder	Grant reference number	Author
Deutsche Forschungsgemeinschaft (DFG)	EXC-2082/1-390761711	Lucie Zilova Joachim Wittbrodt

Author ORCID iDs

Elin Stahl: https://orcid.org/0009-0001-2226-677X
Miguel Angel Delgado-Toscano: https://orcid.org/0000-0001-9128-1511
Ishwariya Saravanan: https://orcid.org/0009-0006-9943-1186
Anastasija Paneva: https://orcid.org/0009-0005-6982-6905

Joachim Wittbrodt: https://orcid.org/0000-0001-8550-7377
Lucie Zilova: https://orcid.org/0000-0001-6404-9119

Additional files

Video S1 Cells of the outer layer of the organoid acquire retina fate, related to Figure 3. Whole volume of day 1 organoid generated form retina-specific *Rx3::H2B-GFP* (50%) reporter line, immunolabeled with anti-GFP antibody, co-stained with DAPI nuclear stain. The percentage (%) indicates the proportion of cells within the organoid carrying indicated reporter. The volume was acquired with 1 µm z step size with confocal microscope Sp8. Scale bar 100 µm.

Video S2 Time laps imaging of multiple organoids from day 1 to day 2 showing the formation of the lens, related to Figure 4. Overlay of brightfield and epifluorescence images of organoids generated from *Foxe3::GFP* (50%) reporter line imaged with the 30 min intervals over 16 h from day 1 (24h post aggregation) to day 2 (40h post aggregation). The percentage (%) indicates the proportion of cells within the organoid carrying indicated reporter. Acquired with ACQUIFER Imaging Machine. Scale bar 100 µm.

Video S3 Lens fate is acquired by cells localized in central part of the organoid, related to Figure 3. Whole volume of day 1 organoid generated form retina-specific *Foxe3::GFP* (50%) reporter line, immunolabeled with anti-GFP antibody, co-stained with DAPI nuclear stain. The percentage (%) indicates the proportion of cells within the organoid carrying indicated reporter. The volume was acquired with 1 µm z step size with confocal microscope Sp8. Scale bar 100 µm.

Video S4 Arrangement of retinal and lens tissue in day 2 organoid, related to Figure 3. Rendering of day 2 organoid generated by mixing of cells from *Rx2::H2B-RFP* (50%) (green) and *Foxe3::GFP* (50%) (magenta) reporter lines immunolabelled with anti-GFP and RFP antibody, co-stained with DAPI nuclear stain (cyan). The percentage (%) indicates the proportion of cells within the organoid carrying indicated reporter. Imaged with Sp8 confocal microscope. Scale bar 100 µm.

Video S5 Re-aggregation of dissociated day 1 organoids, related to Figure 4. Reaggregation of cells generated by dissociation of *Foxe3::GFP* (100%) lens reporter-derived day 1 organoids showing sorting of lens/retinal cell populations imaged with the 1 h intervals over 15 h from day 1 to day 2. Acquired with ACQUIFER Imaging Machine. Scale bar 100 µm.

Video S6 Tracking of movement of individual lens progenitor cells from the center to the periphery of the organoid, related to Figure 4. Organoids derived from *Foxe3::GFP* lens reporter line (10 % of reporter cells with 90 % of wild-type cells) imaged with the 30 min intervals over 10 h from day 1 to day 2. Acquired with ACQUIFER Imaging Machine. Scale bar 100 µm.

Video S7 Cell shape changes of lens-committed progenitor cells during the process of lens displacement from center to the organoid periphery, related to Figure 4. Organoids derived from *Foxe3::GFP* lens reporter line (10 % of reporter cells with 90 % of wild-type cells) imaged with the 30 min intervals over 13 h from day 1 to day 2. Acquired with ACQUIFER Imaging Machine. Scale bar 100 µm; in detail: scale bar 25 µm.

Video S8 Movement or retinal progenitor cells during the process of organoid formation from day 1 to day 2. Organoids derived from *Rx3::H2B-GFP* retinal reporter line (2% of reporter cells with 98 % of wild-type cells) imaged with the 30 min intervals over 13.5 h from day 1 to day 2. Acquired with ACQUIFER Imaging Machine. Scale bar 100 µm.

DataS1 Excel table, related to transcriptome analysis of Figure 7. Normalized and variance stabilized counts labeled with Ensemble IDs.

Figure 4 - Source data 1

Figure 5 - Source data 1

Figure 6 - Source data 1

Figure 2-figure supplement 1 - Source data 1

References

Adelmann H.B. (1937) Experimental studies on the development of the eye. IV. The effect of the partial and complete excision of the prechordal substrate on the development of the eyes of Amblystoma punctatum. *Journal of Experimental Zoology* **75**:199-237 https://doi.org/10.1002/jez.1400750203

Agata K., Kobayashi H., Itoh Y., Mochii M., Sawada K., Eguchi G. (1993) Genetic characterization of the multipotent dedifferentiated state of pigmented epithelial cells in vitro. *Development* **118**:1025-1030 https://doi.org/10.1242/dev.118.4.1025 | PubMed

Agre P., Kozono D. (2003) Aquaporin water channels: molecular mechanisms for human diseases. *FEBS Lett* **555**:72-78 https://doi.org/10.1016/s0014-5793(03)01083-4 | PubMed

Amack J.D., Manning M.L. (2012) Knowing the boundaries: extending the differential adhesion hypothesis in embryonic cell sorting. *Science* **338**:212-215 https://doi.org/10.1126/science.1223953 | PubMed

Bailey A.P., Streit A. (2005) Sensory Organs: Making and Breaking the Pre-Placodal Region. In: *Current Topics in Developmental Biology* Academic Press. pp. 167-204 https://doi.org/10.1016/S0070-2153(05)72003-2 | PubMed

Bassnett S. (2009) On the mechanism of organelle degradation in the vertebrate lens. *Exp Eye Res* **88**:133-139 https://doi.org/10.1016/j.exer.2008.08.017 | PubMed

Bassnett S., Shi Y., Vrensen G.F.J.M. (2011) Biological glass: structural determinants of eye lens transparency. *Philosophical Transactions of the Royal Society B: Biological Sciences* **366**:1250-1264 https://doi.org/10.1098/rstb.2010.0302 | PubMed

Bhattacharyya S., Bailey A.P., Bronner-Fraser M., Streit A. (2004) Segregation of lens and olfactory precursors from a common territory: cell sorting and reciprocity of Dlx5 and Pax6 expression. *Developmental Biology* **271**:403-414 https://doi.org/10.1016/j.ydbio.2004.04.010 | PubMed

Blixt Å., Mahlapuu M., Aitola M., Pelto-Huikko M., Enerbäck S., Carlsson P. (2000) A forkhead gene, FoxE3, is essential for lens epithelial proliferation and closure of the lens vesicle. *Genes Dev* **14**:245-254 https://doi.org/10.1101/gad.14.2.245 | PubMed

Bolger A.M., Lohse M., Usadel B. (2014) Trimmomatic: a flexible trimmer for Illumina sequence data. *Bioinformatics* **30**:2114-2120 https://doi.org/10.1093/bioinformatics/btu170 | PubMed

Brayford S., Kenny F.N., Hiratsuka T., Serna-Morales E., Yolland L., Luchici A., Stramer B.M. (2019) Heterotypic contact inhibition of locomotion can drive cell sorting between epithelial and mesenchymal cell populations. *J Cell Sci* **132**:jcs223974 https://doi.org/10.1242/jcs.223974 | PubMed

Brennan L., Disatham J., Kantorow M. (2021) Mechanisms of organelle elimination for lens development and differentiation. *Exp Eye Res* **209**:108682 https://doi.org/10.1016/j.exer.2021.108682 | PubMed

Brownell I., Dirksen M., Jamrich M. (2000) Forkhead Foxe3 maps to the dysgenetic lens locus and is critical in lens development and differentiation. *Genesis* **27**:81-93 https://doi.org/10.1002/1526-968x(200006)27:2<81::aid-gene50>3.0.co;2-n | PubMed

Camp J.G., Badsha F., Florio M., Kanton S., Gerber T., Wilsch-Bräuninger M., Lewitus E., Sykes A., Hevers W., Lancaster M., *et al.* (2015) Human cerebral organoids recapitulate gene expression programs of fetal neocortex development. *Proceedings of the National Academy of Sciences* **112**:15672-15677 https://doi.org/10.1073/pnas.1520760112 | PubMed

Cardozo M.J., Sánchez-Bustamante E., Bovolenta P. (2023) Optic cup morphogenesis across species and related inborn human eye defects. *Development* **150**:dev200399 https://doi.org/10.1242/dev.200399 | PubMed

Casey M.A., Lusk S., Kwan K.M. (2021) Build me up optic cup: Intrinsic and extrinsic mechanisms of vertebrate eye morphogenesis. *Developmental Biology* **476**:128-136 https://doi.org/10.1016/j.ydbio.2021.03.023 | PubMed

Centanin L., Ander J.-J., Hoeckendorf B., Lust K., Kellner T., Kraemer I., Urbany C., Hasel E., Harris W.A., Simons B.D., *et al.* (2014) Exclusive multipotency and preferential asymmetric divisions in post-embryonic neural stem cells of the fish retina. *Development* **141**:3472-3482 https://doi.org/10.1242/dev.109892 | PubMed

Chaffee B.R., Shang F., Chang M.-L., Clement T.M., Eddy E.M., Wagner B.D., Nakahara M., Nagata S., Robinson M.L., Taylor A. (2014) Nuclear removal during terminal lens fiber cell differentiation requires CDK1 activity: appropriating mitosis-related nuclear disassembly. *Development* **141**:3388-3398 https://doi.org/10.1242/dev.106005 | PubMed

Chen Z., Sugimura R., Zhang Y.S., Ruan C., Wen C. (2024) Organoids in concert: engineering in vitro models toward enhanced fidelity. *Aggregate* **5**:e478 https://doi.org/10.1002/agt2.478

Cheng C., Nowak R.B., Fowler V.M. (2017) The lens actin filament cytoskeleton: Diverse structures for complex functions. *Experimental Eye Research* **156**:58-71 https://doi.org/10.1016/j.exer.2016.03.005 | PubMed

Chow R.L., Lang R.A. (2001) Early Eye Development in Vertebrates. *Annu. Rev. Cell Dev. Biol* **17**:255-296 https://doi.org/10.1146/annurev.cellbio.17.1.255 | PubMed

Chow R.L., Roux G.D., Roghani M., Palmer M.A., Rifkin D.B., Moscatelli D.A., Lang R.A. (1995) FGF suppresses apoptosis and induces differentiation of fibre cells in the mouse lens. *Development* **121**:4383-4393 https://doi.org/10.1242/dev.121.12.4383 | PubMed

Cui X., Wang L., Zhang J., Du R., Liao S., Li D., Li C., Ke T., Li D.W.-C., Huang H., *et al.* (2013) HSF4 regulates DLAD expression and promotes lens de-nucleation. *Biochimica et Biophysica Acta (BBA) - Molecular Basis of Disease* **1832**:1167-1172 https://doi.org/10.1016/j.bbadis.2013.03.007 | PubMed

Cvekl A., Ashery-Padan R. (2014) The cellular and molecular mechanisms of vertebrate lens development. *Development* **141**:4432-4447 https://doi.org/10.1242/dev.107953 | PubMed

Cvekl A., Camerino M.J. (2022) Generation of Lens Progenitor Cells and Lentoid Bodies from Pluripotent Stem Cells: Novel Tools for Human Lens Development and Ocular Disease Etiology. *Cells* **11**:3516 https://doi.org/10.3390/cells11213516 | PubMed

Cvekl A., Duncan M.K. (2007) Genetic and epigenetic mechanisms of gene regulation during lens development. *Prog Retin Eye Res* **26**:555-597 https://doi.org/10.1016/j.preteyeres.2007.07.002 | PubMed

Cvekl A., McGreal R., Liu W. (2015) Chapter Ten - Lens Development and Crystallin Gene Expression. In: Hejtmancik J.F., Nickerson J.M. (Eds). *Progress in Molecular Biology and Translational Science, Molecular Biology of Eye Disease* Academic Press. pp. 129-167 https://doi.org/10.1016/bs.pmbts.2015.05.001 | PubMed

Cvekl A., Zhang X. (2017) Signaling and Gene Regulatory Networks in Mammalian Lens Development. *Trends Genet* **33**:677-702 https://doi.org/10.1016/j.tig.2017.08.001 | PubMed

Davis J.R., Huang C.-Y., Zanet J., Harrison S., Rosten E., Cox S., Soong D.Y., Dunn G.A., Stramer B.M. (2012) Emergence of embryonic pattern through contact inhibition of locomotion. *Development* **139**:4555-4560 https://doi.org/10.1242/dev.082248 | PubMed

Del Bene F., Ettwiller L., Skowronska-Krawczyk D., Baier H., Matter J.-M., Birney E., Wittbrodt J. (2007) In vivo validation of a computationally predicted conserved Ath5 target gene set. *PLoS Genet* **3**:1661-1671 https://doi.org/10.1371/journal.pgen.0030159 | PubMed

Dincer Z., Piao J., Niu L., Ganat Y., Kriks S., Zimmer B., Shi S.-H., Tabar V., Studer L. (2013) Specification of Functional Cranial Placode Derivatives from Human Pluripotent Stem Cells. *Cell Reports* **5**:1387-1402 https://doi.org/10.1016/j.celrep.2013.10.048 | PubMed

Donaldson P.J., Grey A.C., Maceo Heilman B., Lim J.C., Vaghefi E. (2017) The physiological optics of the lens. *Progress in Retinal and Eye Research* **56**:e1-e24 https://doi.org/10.1016/j.preteyeres.2016.09.002 | PubMed

Donaldson P.J., Petrova R.S., Nair N., Chen Y., Schey K.L. (2024) Regulation of water flow in the ocular lens: new roles for aquaporins. *The Journal of Physiology* **602**:3041-3056 https://doi.org/10.1113/JP284102 | PubMed

Dye B.R., Hill D.R., Ferguson M.A., Tsai Y.-H., Nagy M.S., Dyal R., Wells J.M., Mayhew C.N., Nattiv R., Klein O.D., *et al.* (2015) In vitro generation of human pluripotent stem cell derived lung organoids. *eLife* **4**:e05098 https://doi.org/10.7554/eLife.05098 | PubMed

Eagleson G., Ferreiro B., Harris W.A. (1995) Fate of the anterior neural ridge and the morphogenesis of the xenopus forebrain. *Journal of Neurobiology* **28**:146-158 https://doi.org/10.1002/neu.480280203 | PubMed

Eiraku M., Takata N., Ishibashi H., Kawada M., Sakakura E., Okuda S., Sekiguchi K., Adachi T., Sasai Y. (2011) Self-organizing optic-cup morphogenesis in three-dimensional culture. *Nature* **472**:51-56 https://doi.org/10.1038/nature09941 | PubMed

Ershov D., Phan M.-S., Pylvänäinen J.W., Rigaud S.U., Le Blanc L., Charles-Orszag A., Conway J.R.W., Laine R.F., Roy N.H., Bonazzi D., *et al.* (2022) TrackMate 7: integrating state-of-the-art segmentation algorithms into tracking pipelines. *Nat Methods* **19**:829-832 https://doi.org/10.1038/s41592-022-01507-1 | PubMed

Faber S.C., Dimanlig P., Makarenkova H.P., Shirke S., Ko K., Lang R.A. (2001) Fgf receptor signaling plays a role in lens induction. *Development* **128**:4425-4438 https://doi.org/10.1242/dev.128.22.4425 | PubMed

Fu Q., Qin Z., Jin X., Zhang L., Chen Z., He J., Ji J., Yao K. (2017) Generation of Functional Lentoid Bodies From Human Induced Pluripotent Stem Cells Derived From Urinary Cells. *Invest Ophthalmol Vis Sci* **58**:517-527 https://doi.org/10.1167/iovs.16-20504 | PubMed

Fudge D.S., McCuaig J.V., Van Stralen S., Hess J.F., Wang H., Mathias R.T., FitzGerald P.G. (2011) Intermediate Filaments Regulate Tissue Size and Stiffness in the Murine Lens. *Investigative Ophthalmology & Visual Science* **52**:3860-3867 https://doi.org/10.1167/iovs.10-6231 | PubMed

Furuta Y., Hogan B.L.M. (1998) BMP4 is essential for lens induction in the mouse embryo. *Genes Dev* **12**:3764-3775 https://doi.org/10.1101/gad.12.23.3764 | PubMed

Gabriel E., Albanna W., Pasquini G., Ramani A., Josipovic N., Mariappan A., Schinzel F., Karch C.M., Bao G., Gottardo M., *et al.* (2021) Human brain organoids assemble functionally integrated bilateral optic vesicles. *Cell Stem Cell* **28**:1740-1757.e8. https://doi.org/10.1016/j.stem.2021.07.010 | PubMed

Gao M., Huang Y., Wang L., Huang M., Liu F., Liao S., Yu S., Lu Z., Han S., Hu X., *et al.* (2017) HSF4 regulates lens fiber cell differentiation by activating p53 and its downstream regulators. *Cell Death Dis* **8**:e3082-e3082 https://doi.org/10.1038/cddis.2017.478 | PubMed

Greiling T.M.S., Aose M., Clark J.I. (2010) Cell Fate and Differentiation of the Developing Ocular Lens. *Investigative Ophthalmology & Visual Science* **51**:1540-1546 https://doi.org/10.1167/iovs.09-4388 | PubMed

Grocott T., Johnson S., Bailey A.P., Streit A. (2011) Neural crest cells organize the eye via TGF-β and canonical Wnt signalling. *Nat Commun* **2**:265 https://doi.org/10.1038/ncomms1269 | PubMed

Grogg M.W., Call M.K., Okamoto M., Vergara M.N., Del Rio-Tsonis K., Tsonis P.A. (2005) BMP inhibition-driven regulation of six-3 underlies induction of newt lens regeneration. *Nature* **438**:858-862 https://doi.org/10.1038/nature04175 | PubMed

Grün C., Pfeifer J., Liebsch G., Gottwald E. (2023) O2-sensitive microcavity arrays: A new platform for oxygen measurements in 3D cell cultures. *Front. Bioeng. Biotechnol* **11** https://doi.org/10.3389/fbioe.2023.1111316 | PubMed

Gunhaga L. (2011) The lens: a classical model of embryonic induction providing new insights into cell determination in early development. *Philosophical Transactions of the Royal Society B: Biological Sciences* **366**:1193-1203 https://doi.org/10.1098/rstb.2010.0175 | PubMed

Harding R.L., Howley S., Baker L.J., Murphy T.R., Archer W.E., Wistow G., Hyde D.R., Vihtelic T.S. (2008) Lengsin expression and function during zebrafish lens formation. *Experimental Eye Research* **86**:807-818 https://doi.org/10.1016/j.exer.2008.02.009 | PubMed

Hofer M., Lutolf M.P. (2021) Engineering organoids. *Nature Reviews Materials* **6**:402-420 https://doi.org/10.1038/s41578-021-00279-y | PubMed

Iida H., Ishii Y., Kondoh H. (2017) Intrinsic lens potential of neural retina inhibited by Notch signaling as the cause of lens transdifferentiation. *Developmental Biology* **421**:118-125 https://doi.org/10.1016/j.ydbio.2016.11.004 | PubMed

Inoue D., Wittbrodt J. (2011) One for all--a highly efficient and versatile method for fluorescent immunostaining in fish embryos. *PLoS One* **6**:e19713 https://doi.org/10.1371/journal.pone.0019713 | PubMed

Iwamatsu T. (2004) Stages of normal development in the medaka Oryzias latipes. Mechanisms of Development. *Medaka* **121**:605-618 https://doi.org/10.1016/j.mod.2004.03.012 | PubMed

Jarrin M., Pandit T., Gunhaga L. (2012) A balance of FGF and BMP signals regulates cell cycle exit and *Equarin* expression in lens cells. *MBoC* **23**:3266-3274 https://doi.org/10.1091/mbc.e12-01-0075 | PubMed

Kallifatidis G., Boros J., Shin E.H.H., McAvoy J.W., Lovicu F.J. (2011) The fate of dividing cells during lens morphogenesis, differentiation and growth. *Experimental Eye Research* **92**:502-511 https://doi.org/10.1016/j.exer.2011.03.012 | PubMed

Kamachi Y., Uchikawa M., Collignon J., Lovell-Badge R., Kondoh H. (1998) Involvement of Sox1, 2 and 3 in the early and subsequent molecular events of lens induction. *Development* **125**:2521-2532 https://doi.org/10.1242/dev.125.13.2521 | PubMed

Kenyon K.L., Zaghloul N., Moody S.A. (2001) Transcription factors of the anterior neural plate alter cell movements of epidermal progenitors to specify a retinal fate. *Dev Biol* **240**:77-91 https://doi.org/10.1006/dbio.2001.0464 | PubMed

Klimova L., Kozmik Z. (2014) Stage-dependent requirement of neuroretinal Pax6 for lens and retina development. *Development* **141**:1292-1302 https://doi.org/10.1242/dev.098822 | PubMed

Kreslova J., Machon O., Ruzickova J., Lachova J., Wawrousek E.F., Kemler R., Krauss S., Piatigorsky J., Kozmik Z. (2007) . Abnormal lens morphogenesis and ectopic lens formation in the absence of β-catenin function. *genesis* **45**:157-168 https://doi.org/10.1002/dvg.20277 | PubMed

Kretzschmar K., Clevers H. (2016) Organoids: Modeling Development and the Stem Cell Niche in a Dish. *Developmental Cell* **38**:590-600 https://doi.org/10.1016/j.devcel.2016.08.014 | PubMed

Krieg M., Arboleda-Estudillo Y., Puech P.-H., Käfer J., Graner F., Müller D.J., Heisenberg C.-P. (2008) Tensile forces govern germ-layer organization in zebrafish. *Nat Cell Biol* **10**:429-436 https://doi.org/10.1038/ncb1705 | PubMed

Kuwahara A., Ozone C., Nakano T., Saito K., Eiraku M., Sasai Y. (2015) Generation of a ciliary margin-like stem cell niche from self-organizing human retinal tissue. *Nature Communications* **6**:6286 https://doi.org/10.1038/ncomms7286 | PubMed

Lancaster M.A., Renner M., Martin C.-A., Wenzel D., Bicknell L.S., Hurles M.E., Homfray T., Penninger J.M., Jackson A.P., Knoblich J.A. (2013) Cerebral organoids model human brain development and microcephaly. *Nature* **501**:373-379 https://doi.org/10.1038/nature12517 | PubMed

Lang R.A. (2004) Pathways regulating lens induction in the mouse. *Int J Dev Biol* **48**:783-791 https://doi.org/10.1387/ijdb.041903rl | PubMed

Langmead B., Salzberg S.L. (2012) Fast gapped-read alignment with Bowtie 2. *Nat Methods* **9**:357-359 https://doi.org/10.1038/nmeth.1923 | PubMed

Le A.C., Musil L.S. (2001) FGF signaling in chick lens development. *Dev Biol* **233**:394-411 https://doi.org/10.1006/dbio.2001.0194 | PubMed

Leung A.W., Morest D.K., Li J.Y.H. (2013) Differential BMP signaling controls formation and differentiation of multipotent preplacodal ectoderm progenitors from human embryonic stem cells. *Dev Biol* **379**:208-220 https://doi.org/10.1016/j.ydbio.2013.04.023 | PubMed

Li H., Tierney C., Wen L., Wu J.Y., Rao Y. (1997) A single morphogenetic field gives rise to two retina primordia under the influence of the prechordal plate. *Development* **124**:603-615 https://doi.org/10.1242/dev.124.3.603 | PubMed

Liao Y., Smyth G.K., Shi W. (2014) featureCounts: an efficient general purpose program for assigning sequence reads to genomic features. *Bioinformatics* **30**:923-930 https://doi.org/10.1093/bioinformatics/btt656 | PubMed

Litsiou A., Hanson S., Streit A. (2005) A balance of FGF, BMP and WNT signalling positions the future placode territory in the head. *Development* **132**:4051-4062 https://doi.org/10.1242/dev.01964 | PubMed

Loosli F., Köster R.W., Carl M., Kühnlein R., Henrich T., Mücke M., Krone A., Wittbrodt J. (2000) A genetic screen for mutations affecting embryonic development in medaka fish (Oryzias latipes). *Mechanisms of Development* **97**:133-139 https://doi.org/10.1016/S0925-4773(00)00406-8 | PubMed

Love M.I., Huber W., Anders S. (2014) Moderated estimation of fold change and dispersion for RNA-seq data with DESeq2. *Genome Biology* **15**:550 https://doi.org/10.1186/s13059-014-0550-8 | PubMed

Lovicu F.J., McAvoy J.W. (2005) Growth factor regulation of lens development. *Dev Biol* **280**:1-14 https://doi.org/10.1016/j.ydbio.2005.01.020 | PubMed

Maki N., Takechi K., Sano S., Tarui H., Sasai Y., Agata K. (2007) Rapid accumulation of nucleostemin in nucleolus during newt regeneration. *Developmental Dynamics* **236**:941-950 https://doi.org/10.1002/dvdy.21027 | PubMed

Mathers P.H., Grinberg A., Mahon K.A., Jamrich M. (1997) The Rx homeobox gene is essential for vertebrate eye development. *Nature* **387**:603-607 https://doi.org/10.1038/42475 | PubMed

Mathias R.T., White T.W., Gong X. (2010) Lens gap junctions in growth, differentiation, and homeostasis. *Physiol Rev* **90**:179-206 https://doi.org/10.1152/physrev.00034.2009 | PubMed

McAvoy J.W., Chamberlain C.G., de Iongh R.U., Hales A.M., Lovicu F.J. (1999) Lens development. *Eye* **13**:425-437 https://doi.org/10.1038/eye.1999.117 | PubMed

McCabe K.L., Bronner-Fraser M. (2009) Molecular and tissue interactions governing induction of cranial ectodermal placodes. *Developmental Biology* **332**:189-195 https://doi.org/10.1016/j.ydbio.2009.05.572 | PubMed

McCracken K.W., Catá E.M., Crawford C.M., Sinagoga K.L., Schumacher M., Rockich B.E., Tsai Y.-H., Mayhew C.N., Spence J.R., Zavros Y., *et al.* (2014) Modelling human development and disease in pluripotent stem-cell-derived gastric organoids. *Nature* **516**:400-404 https://doi.org/10.1038/nature13863 | PubMed

McMurtrey R.J. (2016) Analytic Models of Oxygen and Nutrient Diffusion, Metabolism Dynamics, and Architecture Optimization in Three-Dimensional Tissue Constructs with Applications and Insights in Cerebral Organoids. *Tissue Engineering Part C: Methods* **22**:221-249 https://doi.org/10.1089/ten.tec.2015.0375 | PubMed

Mellough C.B., Collin J., Khazim M., White K., Sernagor E., Steel D.H.W., Lako M. (2015) IGF-1 Signaling Plays an Important Role in the Formation of Three-Dimensional Laminated Neural Retina and Other Ocular Structures From Human Embryonic Stem Cells. *Stem Cells* **33**:2416-2430 https://doi.org/10.1002/stem.2023 | PubMed

Mikula Mrstakova S., Kozmik Z. (2024) Genetic analysis of medaka fish illuminates conserved and divergent roles of Pax6 in vertebrate eye development. *Front. Cell Dev. Biol* **12** https://doi.org/10.3389/fcell.2024.1448773 | PubMed

Morishita H., Eguchi T., Tsukamoto S., Sakamaki Y., Takahashi S., Saito C., Koyama-Honda I., Mizushima N. (2021) Organelle degradation in the lens by PLAAT phospholipases. *Nature* **592**:634-638 https://doi.org/10.1038/s41586-021-03439-w | PubMed

Nakano T., Ando S., Takata N., Kawada M., Muguruma K., Sekiguchi K., Saito K., Yonemura S., Eiraku M., Sasai Y. (2012) Self-formation of optic cups and storable stratified neural retina from human ESCs. *Cell Stem Cell* **10**:771-785 https://doi.org/10.1016/j.stem.2012.05.009 | PubMed

Ogino H., Ochi H., Reza H.M., Yasuda K. (2012) Transcription factors involved in lens development from the preplacodal ectoderm. *Dev Biol* **363**:333-347 https://doi.org/10.1016/j.ydbio.2012.01.006 | PubMed

Ogino H., Yasuda K. (2000) Sequential activation of transcription factors in lens induction. *Dev Growth Differ* **42**:437-448 https://doi.org/10.1046/j.1440-169x.2000.00532.x | PubMed

Okada T.S., Itoh Y., Watanabe K., Eguchi G. (1975) Differentiation of lens in cultures of neural retinal cells of chick embryos. *Developmental Biology* **45**:318-329 https://doi.org/10.1016/0012-1606(75)90069-X | PubMed

Pandey G., Westhoff J.H., Schaefer F., Gehrig J. (2019) A Smart Imaging Workflow for Organ-Specific Screening in a Cystic Kidney Zebrafish Disease Model. *Int J Mol Sci* **20**:1290 https://doi.org/10.3390/ijms20061290 | PubMed

Perng M.-D., Zhang Q., Quinlan R.A. (2007) Insights into the beaded filament of the eye lens. *Experimental Cell Research* **313**:2180-2188 https://doi.org/10.1016/j.yexcr.2007.04.005 | PubMed

Pistocchi A., Gaudenzi G., Carra S., Bresciani E., Del Giacco L., Cotelli F. (2008) Crucial role of zebrafish prox1in hypothalamic catecholaminergic neurons development. *BMC Developmental Biology* **8**:27 https://doi.org/10.1186/1471-213X-8-27 | PubMed

Porter F.D., Drago J., Xu Y., Cheema S.S., Wassif C., Huang S.P., Lee E., Grinberg A., Massalas J.S., Bodine D., *et al.* (1997) Lhx2, a LIM homeobox gene, is required for eye, forebrain, and definitive erythrocyte development. *Development* **124**:2935-2944 https://doi.org/10.1242/dev.124.15.2935 | PubMed

Qian X., Song H., Ming G. (2019) Brain organoids: advances, applications and challenges. *Development* **146**:dev166074 https://doi.org/10.1242/dev.166074 | PubMed

Rajagopal R., Huang J., Dattilo L.K., Kaartinen V., Mishina Y., Deng C.-X., Umans L., Zwijsen A., Roberts A.B., Beebe D.C. (2009) The type I BMP receptors, Bmpr1a and Acvr1, activate multiple signaling pathways to regulate lens formation. *Developmental Biology* **335**:305-316 https://doi.org/10.1016/j.ydbio.2009.08.027 | PubMed

Rao P.V., Maddala R. (2006) The role of the lens actin cytoskeleton in fiber cell elongation and differentiation. *Seminars in Cell & Developmental Biology, TRP Channels* **17**:698-711 https://doi.org/10.1016/j.semcdb.2006.10.011 | PubMed

Reinhardt R., Centanin L., Tavhelidse T., Inoue D., Wittbrodt B., Concordet J., Martinez-Morales J.R., Wittbrodt J. (2015) Sox2, Tlx, Gli3, and Her9 converge on Rx2 to define retinal stem cells in vivo. *The EMBO Journal* **34**:1572-1588 https://doi.org/10.15252/embj.201490706 | PubMed

Rembold M., Loosli F., Adams R.J., Wittbrodt J. (2006) Individual Cell Migration Serves as the Driving Force for Optic Vesicle Evagination. *Science* **313**:1130-1134 https://doi.org/10.1126/science.1127144 | PubMed

Robinson M.L. (2006) An essential role for FGF receptor signaling in lens development. *Semin Cell Dev Biol* **17**:726-740 https://doi.org/10.1016/j.semcdb.2006.10.002 | PubMed

Sahu S., Sharan S.K. (2020) Translating Embryogenesis to Generate Organoids: Novel Approaches to Personalized Medicine. *iScience* **23**:101485 https://doi.org/10.1016/j.isci.2020.101485 | PubMed

Schindelin J., Arganda-Carreras I., Frise E., Kaynig V., Longair M., Pietzsch T., Preibisch S., Rueden C., Saalfeld S., Schmid B., *et al.* (2012) Fiji: an open-source platform for biological-image analysis. *Nat Methods* **9**:676-682 https://doi.org/10.1038/nmeth.2019 | PubMed

Schlosser G. (2006) Induction and specification of cranial placodes. *Dev Biol* **294**:303-351 https://doi.org/10.1016/j.ydbio.2006.03.009 | PubMed

Shi X., Luo Y., Howley S., Dzialo A., Foley S., Hyde D.R., Vihtelic T.S. (2006) Zebrafish *foxe3*: Roles in ocular lens morphogenesis through interaction with *pitx3*. *Mechanisms of Development* **123**:761-782 https://doi.org/10.1016/j.mod.2006.07.004 | PubMed

Sjödal M., Edlund T., Gunhaga L. (2007) Time of Exposure to BMP Signals Plays a Key Role in the Specification of the Olfactory and Lens Placodes Ex Vivo. *Developmental Cell* **13**:141-149 https://doi.org/10.1016/j.devcel.2007.04.020 | PubMed

Smith T., Heger A., Sudbery I. (2017) UMI-tools: modeling sequencing errors in Unique Molecular Identifiers to improve quantification accuracy. *Genome Res* **27**:491-499 https://doi.org/10.1101/gr.209601.116 | PubMed

Song S., Landsbury A., Dahm R., Liu Y., Zhang Q., Quinlan R.A. (2009) Functions of the intermediate filament cytoskeleton in the eye lens. *J Clin Invest* **119**:1837-1848 https://doi.org/10.1172/JCI38277 | PubMed

Steinberg M.S. (1963) Reconstruction of tissues by dissociated cells. Some morphogenetic tissue movements and the sorting out of embryonic cells may have a common explanation. *Science* **141**:401-408 https://doi.org/10.1126/science.141.3579.401 | PubMed

Thermes V., Grabher C., Ristoratore F., Bourrat F., Choulika A., Wittbrodt J., Joly J.-S. (2002) *I-SceI* meganuclease mediates highly efficient transgenesis in fish. *Mechanisms of Development* **118**:91-98 https://doi.org/10.1016/S0925-4773(02)00218-6 | PubMed

Toro S., Varga Z.M. (2007) Equivalent progenitor cells in the zebrafish anterior preplacodal field give rise to adenohypophysis, lens, and olfactory placodes. Seminars in Cell & Developmental Biology. *Coat Proteins and Coated Vesicles* **18**:534-542 https://doi.org/10.1016/j.semcdb.2007.04.003 | PubMed

Tse H.M., Gardner G., Dominguez-Bendala J., Fraker C.A. (2021) The Importance of Proper Oxygenation in 3D Culture. *Front. Bioeng. Biotechnol* **9** https://doi.org/10.3389/fbioe.2021.634403 | PubMed

Varadaraj K., Kushmerick C., Baldo G.J., Bassnett S., Shiels A., Mathias R.T. (1999) The role of MIP in lens fiber cell membrane transport. *J Membr Biol* **170**:191-203 https://doi.org/10.1007/s002329900549 | PubMed

Vining K.H., Mooney D.J. (2017) Mechanical forces direct stem cell behaviour in development and regeneration. *Nat Rev Mol Cell Biol* **18**:728-742 https://doi.org/10.1038/nrm.2017.108 | PubMed

Völkner M., Zschätzsch M., Rostovskaya M., Overall R.W., Busskamp V., Anastassiadis K., Karl M.O. (2016) Retinal Organoids from Pluripotent Stem Cells Efficiently Recapitulate Retinogenesis. *Stem Cell Reports* **6**:525-538 https://doi.org/10.1016/j.stemcr.2016.03.001 | PubMed

Wawersik S., Purcell P., Rauchman M., Dudley A.T., Robertson E.J., Maas R. (1999) BMP7 acts in murine lens placode development. *Dev Biol* **207**:176-188 https://doi.org/10.1006/dbio.1998.9153 | PubMed

Wigle J.T., Chowdhury K., Gruss P., Oliver G. (1999) Prox1 function is crucial for mouse lens-fibre elongation. *Nat Genet* **21**:318-322 https://doi.org/10.1038/6844 | PubMed

Wride M.A. (2011) Lens fibre cell differentiation and organelle loss: many paths lead to clarity. *Philos Trans R Soc Lond B Biol Sci* **366**:1219-1233 https://doi.org/10.1098/rstb.2010.0324 | PubMed

Yang C., Yang Y., Brennan L., Bouhassira E.E., Kantorow M., Cvekl A. (2010) Efficient generation of lens progenitor cells and lentoid bodies from human embryonic stem cells in chemically defined conditions. *FASEB J* **24**:3274-3283 https://doi.org/10.1096/fj.10-157255 | PubMed

Zhang Jing, Cui W.-W., Du C., Huang Y., Pi X., Guo W., Wang J., Huang W., Chen D., Li J., *et al.* (2020) Knockout of DNase1l1l abrogates lens denucleation process and causes cataract in zebrafish. *Biochim Biophys Acta Mol Basis Dis* **1866**:165724 https://doi.org/10.1016/j.bbadis.2020.165724 | PubMed

Zhang Y., Thomas G.L., Swat M., Shirinifard A., Glazier J.A. (2011) Computer Simulations of Cell Sorting Due to Differential Adhesion. *PLoS One* **6**:e24999 https://doi.org/10.1371/journal.pone.0024999 | PubMed

Zhao H., Yang T., Madakashira B.P., Thiels C.A., Bechtle C.A., Garcia C.M., Zhang H., Yu K., Ornitz D.M., Beebe D.C., *et al.* (2008) Fibroblast growth factor receptor signaling is essential for lens fiber cell differentiation. *Dev Biol* **318**:276-288 https://doi.org/10.1016/j.ydbio.2008.03.028 | PubMed

Zhao Z., Chen X., Dowbaj A.M., Sljukic A., Bratlie K., Lin L., Fong E.L.S., Balachander G.M., Chen Z., Soragni A., *et al.* (2022) Organoids. *Nat Rev Methods Primers* **2**:1-21 https://doi.org/10.1038/s43586-022-00174-y | PubMed

Zhou M., Leiberman J., Xu J., Lavker R.M. (2006) A Hierarchy of Proliferative Cells Exists in Mouse Lens Epithelium: Implications for Lens Maintenance. *Investigative Ophthalmology & Visual Science* **47**:2997-3003 https://doi.org/10.1167/iovs.06-0130 | PubMed

Zhu X., Huang L., Zheng Y., Song Y., Xu Q., Wang J., Si K., Duan S., Gong W. (2019) Ultrafast optical clearing method for three-dimensional imaging with cellular resolution. *Proc Natl Acad Sci U S A* **116**:11480-11489 https://doi.org/10.1073/pnas.1819583116 | PubMed

Zilova L., Weinhardt V., Tavhelidse T., Schlagheck C., Thumberger T., Wittbrodt J. (2021) Fish primary embryonic pluripotent cells assemble into retinal tissue mirroring in vivo early eye development. *eLife* **10**:e66998 https://doi.org/10.7554/eLife.66998 | PubMed

Stahl E, Delgado-Toscano MA, Saravanan I, Paneva A, Joachim W, Zilova L (2026) Transcriptome analysis of medaka embryonic eye and ocular organoids [data]. heiDATA. https://doi.org/10.11588/DATA/VEREK9

Peer reviews

Reviewer #1 (Public review):

Summary:

The authors focused on medaka retinal organoids to investigate the mechanism underlying the eye cup morphogenesis. The authors succeeded to induce lens formation in fish retinal organoids using 3D suspension culture with minimal growth factor-containing media containing the Hepes. At day 1, retinal precursor cells expressing Rx3:H2B-GFP appear in the surface region of organoids. At day 1.5, Prox1+ cells appear in the interface area between the organoid surface and the core of central cell mass, which develops a spherical-shaped lens later. So, Prox1+ cells covers the surface of the internal lens cell core. At day 2, foxe3:GFP+ cells appear in the Prox1+ area, where early lens fiber marker, LFC, starts to be expressed. In addition, foxe3:GFP+ cells show EdU+ incorporation, indicating that foxe3:GFP+ cells have lens epithelial cell-characters. At day 4, cry:EGFP+ cells differentiate inside the spherical lens core, whose surface area consists of LFC+ and Prox1+ cells. Furthermore, at day 4, the lens core moves towards the surface of retinal organoids to form an eyecup like structure, although this morphogenesis "inside out" mechanism is different from in vivo cellular "outside -in" mechanism of eye cup formation. From these data, the authors conclude that optic cup formation, especially the positioning of the lens, is established in retinal organoids though the different mechanism of in vivo morphogenesis.

In the revised manuscript, the authors have added new data on dissociation and re-aggregation of day one organoids and revealed that differentially adhesive property of lens and retinal precursors cells enables the formation of a spherical lens in the center of the organoid and later movement of lens toward the peripheral region of the organoid for lens evagination. Furthermore, the authors showed that BMP and FGF signaling are required for lens precursor induction and subsequent lens fiber differentiation in the organoid, respectively. In the revised manuscript, they have added new data on target tissue of BMP and FGF signaling pathways by showing phosphorylated Smad1/5/8 and phosphorylated ERK1/2, respectively, and revealed that lens precursor cells formed in the center of day one organoid are target of BMP signaling, whereas lens fiber cells formed in the center of day 1.5 to 2 organoid are targeted by FGF signaling. Finally, the authors conducted bulk RNA-seq analysis of 1-4 dpf embryonic eyes and day 1-4 eye organoids and revealed that lens organoids show a similar temporal profile of gene transcription. These data suggest that,

although induction and morphogenesis of lens are differentially regulated between eye organoids and in vivo embryonic eyes, their molecular mechanism seems to be shared.

Significance:

Strength: This study is unique. The authors examined eye cup morphogenesis using fish retinal organoids. Eye cup normally consists of the lens, the neural retina, pigment epithelium and optic stalk. However, retinal organoids seem to be simple and consists of two cell types, lens and retina. Interestingly, a similar optic cup-like structure is achieved in both cases; however, cellular mechanism of lens induction and morphogenesis are different between retinal organoid and in vivo eyes, although their molecular mechanism is conserved.

Limitation: In the revised manuscript, the authors clarified almost obscure points; however, a couple of unclear points are still retained. First, there is one unknown cell-type population located in the interface area between foxe3:GFP+ cells and rx2:H2B-RFP+ cells at day 2 organoid. Second, the authors showed that removal of HEPES from the organoid culture media inhibits lens induction and differentiation. However, the role of HEPES in lens induction and differentiation in the organoid remains to be elucidated.

Advancement: In the revised manuscript, the authors have provided precise description of inductive and morphogenetic process of lens induction and differentiation in retinal organoid as well as their molecular evidence, which impact the research field of cell biology and regenerative medical science using human organoid.

Audience: The target audience of current study are still within ophthalmology and neuroscience community people, maybe translational/clinical rather than basic biology. To beyond specific fields, need to formulate a general principle for cell and developmental biology.

https://doi.org/10.7554/eLife.108702.2.sa3

Reviewer #2 (Public review):

Summary:

In this study from Stahl et al., the authors demonstrate that medaka pluripotent embryonic cells can self-organise into eye organoids containing both retina and lens tissues. While these organoids can self-organize into an eye structure that resembles the vertebrate eye, they are built from a fundamentally different morphogenetic process - an "inside-out" mechanism where the lens forms centrally and moves outward, rather than the normal "outside-in" embryonic process. This is a very interesting discovery, both for our understanding of developmental biology and the potential for tissue engineering applications. The study would benefit from some additional experiments and a few clarifications. The authors suggest that the lens cells are the ones that move from the central to a more superficial position. Is this an active movement of lens cells or just the passive consequence of the retina cells acquiring a cup shape? Are the retina cells migrating behind the lens or the lens cells pushing outwards? High-resolution imaging of organoid cup formation, tracking retina cells in combination with membrane labeling of all cells would help elucidate the morphogenetic processes occurring in the organoids. Membrane labeling would also be useful as Prox1 positive lens cells appear elongated in embryos while in the organoids, cell shapes seem less organised, less compact and not elongated (for example as shown in Fig 3f,g).

The organoids could be a useful tool to address how cell fate is linked to cell shape acquisition. In the forming organoids, retinal tissue initially forms on the outside, while non-retinal tissue is located in the centre; this central tissue later expresses lens markers. Do the

authors have any insights into why fate acquisition occurs in this pattern? Is there a difference in proliferation rates between the centrally located cells and the external ones? Could it be that highly proliferative cells give rise to neural retina (NR), while lower proliferating cells become lens?

What happens in organoids that do not form lenses? Do these organoids still generate foxe3 positive cells that fail to develop into a proper lens structure? And in the absence of lens formation, does the retina still acquire a cup shape?

The author suggest that lens formation occurs even in the absence of Matrigel. Is the process slower in these conditions? Are the resulting organoids smaller? While there are indeed some LFC expressing cells by day2, these cells are not very well organised and the pattern of expression seems dotty. Moreover, LFC staining seems to localise posterior to the LFC negative, lens-like structure (e.g. Fig.S1 3o'clock).

How do these organoids develop beyond day 4? Do they maintain their structural integrity at later stages?

The role of HEPES in promoting organoid formation is intriguing. Do the authors have any insights into why it is important in this context? Have the authors tried other culture conditions and does culture condition influence the morphogenetic pathways occurring within the organoids?

Significance:

This is a very interesting paper, and it will be important to determine whether this alternative morphogenetic process is specific to medaka or if similar developmental routes can be recapitulated in organoid cultures from other vertebrate species.

Comments on revised version:

The revised manuscript is much improved and addresses all of the points raised by the reviewers.

https://doi.org/10.7554/eLife.108702.2.sa2

Reviewer #3 (Public review):

Major Comments on first version:

- The manuscript presents a beautiful set of high-quality images showing expression of lens differentiation markers over time in the organoids. The set of experiments is very robust, with high numbers of organoids analysed and reproducible data. The mechanism by which lens specification is promoted in these organoids is, however, poorly analysed, and the reader does not get a clear understanding of what is different in these experiments, as compared to previous attempts, to support lens differentiation. There is a mention to HEPES supplementation, but no further analysis is provided, and the fact that the process is independent of ECM contradicts, as the authors point out, previous reports. The manuscript would benefit from a more detailed analysis of the mechanisms that lead to lens differentiation in this setting.

- The markers analysed to show onset of lens differentiation in the organoids seem to start being expressed, in vivo, when the lens placode starts invaginating. An analysis of earlier stages is not presented. This would be very informative, allowing to determine whether progenitors differentiate as placode and neuroepithelium first, to subsequently continue differentiating into lens and retina, respectively. Could early placodal and anterior neural

plate markers be analysed in the organoids? This would provide a more complete sequence of lens vs retina differentiation in this model.

- The analysis of BMP and Fgf requirement for lens formation and differentiation is suggestive, but the source of these signals is not resolved or mentioned in the manuscript. Are BMP4 and Fgf8 expressed by the organoids? Where are they coming from?

- The fact that the lens becomes specified in the centre of the organoid is striking, but it is for me difficult to visualise how it ends up being extruded from the organoid. Did the authors try to follow this process in movies? I understand that this may be technically challenging, but it would certainly help to understand the process that leads to the final organisation of retinal and lens tissues in the organoid. There is no discussion of why the morphogenetic mechanism is so different from the in vivo situation. The manuscript would benefit from explicitly discussing this.

Significance:

This study describes a reproducible approach to differentiate ocular organoids composed of lens and retinal tissues. The characterisation of lens differentiation in this model is very detailed, and despite the morphogenetic differences, the molecular mechanisms show many similarities to the in vivo situation. The manuscript however does not highlight, in my opinion, why this model may be relevant. Clearly articulating this relevance, particularly in the discussion, will enhance the study and provide more clarity to the readers regarding the significance of the study for the field of organoid research, ocular research and regenerative studies.

Comments on revised version:

The authors presented substantial additional experimental evidence that further strengthens their manuscript and addressed with these experiments and their revised results/discussion in the manuscript the comments and suggestions from the reviewers. I think the manuscript has been greatly improved with the additions presented.

https://doi.org/10.7554/eLife.108702.2.sa1

Author response:

The following is the authors' response to the original reviews

Thank you very much for the positive and constructive feedback on our manuscript. We have revised the manuscript accordingly and have added a substantial number of additional experiments and have extended the data.

Questions of the reviewers were focused mostly on mechanical insight into organoid formation, touching following aspects of lens organoid formation presented in the manuscript:

- Cellular arrangements/re-arrangements during the process of lens formation including potential contribution of differential adhesion-mediated cell sorting to the cellular arrangement in the organoid and characterization of individual contributions of lens- and retina- committed progenitors to this process.

- Activity of BMP and FGF signaling pathways during organoid formation, namely identification of tissue responding to the signaling withing forming organoids.

- Contribution of externally supplemented Matrigel to the differentiation process and cellular arrangements in ocular organoids.

To address those points in detail we included additional experiments that are now presented in revised version of the manuscript, namely in revised Figure 2-figure supplement 1 (addressing contribution of Matrigel); new Figure 4-supplement 1/Video S5 (addressing contribution of differential adhesion-mediated cell sorting); revised Figure 4/Video S6/Video S7 (addressing contribution of lens-committed progenitors); revised Figure 6 (addressing BMP and FGF signaling pathway activities).

> ***Reviewer #1 (Evidence, reproducibility and clarity):***
>
> *Summary*
>
> *The authors focused on medaka retinal organoids to investigate the mechanism underlying the eye cup morphogenesis. The authors succeeded to induce lens formation in fish retinal organoids using 3D suspension culture with minimal growth factor-containing media containing the Hepes. At day 1, Rx3:H2B-GFP + cells appear in the surface region of organoids. At day 1.5, Prox1+cells appear in the interface area between the organoid surface and the core of central cell mass, which develops a spherical-shaped lens later. So, Prox1+ cells covers the surface of the internal lens cell core. At day 2, foxe3:GFP+ cells appear in the Prox1+ area, where early lens fiber marker, LFC, starts to be expressed. In addition, foxe3:GFP+ cells show EdU+ incorporation, indicating that foxe3:GFP+ cells have lens epithelial cell-characters. At day 4, cry:EGFP+ cells differentiate inside the spherical lens core, whose the surface area consists of LFC+ and Prox1+ cells. Furthermore, at day 4, the lens core moves towards the surface of retinal organoids to form an eye-cup like structure, although this morphogenesis "inside out" mechanism is different from in vivo cellular "outside -in" mechanism of eye cup formation. From these data, the authors conclude that optic cup formation, especially the positioning of the lens, is established in retinal organoids though the different mechanism of in vivo morphogenesis.*
>
> *Overall, manuscript presentation is nice. However, there are still obscure points to understand background mechanism. My comments are shown below.*
>
> *Major comments*
>
> *(1) At the initial stage of retinal organoid morphogenesis, a spherical lens is centrally positioned inside the retinal organoids, by covering a central lens core by the outer cell sheet of retinal precursor cells. I wonder if the formation of this structure may be understood by differential cell adhesive activity or mechanical tension between lens core cells and retinal cell sheet, just like the previous study done by Heisenberg lab on the spatial patterning of endoderm, mesoderm and ectoderm (Nat. Cell Biol. 10, 429 - 436 (2008)). Lens core cells may be integrated inside retinal cell mass by cell sorting through the direct interaction between retinal cells and lens cells, or between lens cells and the culture media. After day 1, it is also possible to understand that lens core moves towards the surface of retinal organoids, if adhesive/tensile force states of lens core cells may be change by secretion of extracellular matrix. I wonder if the authors measure physical property, adhesive activity and solidness, of retinal precursor cells and lens core cells. If retinal organoids at day 1 are dissociated and cultured again, do they show the same patterning of internal lens core covering by the outer retinal cell sheet?*

The question, whether different adhesive activity is involved in cell sorting and lens formation is indeed very intriguing.

To address this point, we included additional experiments in the revised manuscript. As proposed by the reviewer, we performed dissociation and re-aggregation experiments of day one organoids at the timepoint, when retinal cell fate is already established and first cells

with early lens fate (Foxe3::GFP positive) start appearing (see new Figure 4-figure supplement 1).

After dissociation we followed Foxe3::GFP cells over time and observed that initially equally dispersed GFP$^+$ lens-committed cells gradually sort and establish contact with other GFP$^+$ cells, ultimately resulting in the formation of a central GFP$^+$ sphere within a retinal neuroepithelium (AcTub$^+$) localized on the surface of the organoid (see new Figure 4-figure supplement 1e and new Video S5). This data show that differential adhesive properties of lens/retinal precursor cells can enable the formation of a spherical lens in the center of the organoid. This is now clearly stated in the revised version of the manuscript.

> *(2) Optic cup is evaginated from the lateral wall of neuroepithelium of the diencephalon. In zebrafish, cell movement occurs from the pigment epithelium to the neural retina during eye morphogenesis in an FGF-dependent manner. How the medaka optic cup morphogenesis is coordinated? I also wonder if the authors conduct the tracking of cell migration during optic cup morphogenesis to reveal how cell migration and cell division are regulated in lens of the Medaka retinal organoids. It is also interesting to examine how retinal cell movement is coordinated during Medaka retinal organoids.*

Looking into the detail of how optic cup-looking tissue arrangement of ocular organoids is achieved on cellular level is of course interesting. Our previous study showed that optic vesicles of medaka retinal organoids do not form optic cups (for details please see Zilova et al., 2021, eLife). We provide evidence that the formation of cup-looking structure of the ocular organoids presented here is mediated by the following processes: establishment of retina and lens domains at specific regions of the organoid – retina on the surface and lens in the center (see Figure 3-figure supplement 1d and Figure 3e, and Figure 4). Further, the dislocation of the centrally formed lens towards the organoid periphery results in the opening of the retina layer, moving the lens to the periphery while retinal cells stay static. We propose that the “cup-like” shape is acquired by an extrusion-like process of the lens from the center of the organoid.

To address the cellular mechanisms involved in this process, we included additional experiments and followed the movements of retinal and lens cells (see new Figure 4c and 4d, new Videos S6, S7 and S8). Retinal cells (tracked as nuclei of the Rx3::H2B-GFP transgenic line) established in the periphery display repeated short distance movements restricted to the retinal epithelium. These movements are characteristic for interkinetic nuclear migration as found in the developing retina. In contrast, Foxe3::GFP lens progenitor cells performed long distance movements from the center to the periphery of the organoid. This movement was accompanied by profound cell shape changes of lens progenitor cells, suggesting an active movement of lens cells to the organoid periphery. These movements are shown in new/extended figures and in new supplementary videos (new Figure 4c and 4d, new Videos S6, S7 and S8) in the revised version of the manuscript.

> *(3) The authors showed that blockade of FGF signaling affects lens fiber differentiation in day 1-2, whereas lens formation seems to be intact in the presence of FGF receptor inhibitor in day 0-1. I suggest the authors to examine which tissue is a target of FGF signaling in retinal organoids, using markers such as pea3, which is a downstream target of ERK branch of FGF signaling. Since FGF signaling promotes cell proliferation, is the lens core size normal in SU5402-treated organoids from day 0 to day 1?*

Assessing the activity of FGF signaling (cross-reference to Reviewer #3) in the organoids is an important point that we have taken care of and included in the revised manuscript.

To address this point, we assessed which tissue/part of the organoid is responding to FGF signaling. To do so we analyzed the presence of phosphorylated ERK (pERK1/2) as FGF signaling target in ocular organoids from day 1 to day 2. At day 1, only low levels of FGF

signaling activity were detectable in presumptive retinal or/and lens tissue (see revised Figure 6b). Only half a day later, a significant increase in FGF activity was observed specifically in the central region of the organoids (lens progenitor domain) (at day 1.5), prior to the onset of differentiation of lens fiber cells. This, together with inability of lens progenitor cells to differentiate to lens fiber cells in the presence of FGF inhibitor SU5402 provided during this critical period (day 1 to day 2) demonstrates that FGF signaling activity localized in the lens progenitor cells is required for lens fiber differentiation.

By day 2, FGF activity was detected in both lens and retinal tissue of the organoid. Similar patterns of FGF activity were observed in embryos at 2 days post fertilization (see revised Figure 6b).

The treatment with the FGF signaling inhibitor SU5402 from day 0 to day 1 did have no impact on the core size of organoid the dimension of which were fully comparable to the control (please see Figure 6d).

> *(4) Fig. 3f and 3g indicate that there is some cell population located between foxe3:GFP+ cells and rx2:H2B-RFP+ cells. What kind of cell-type is occupied in the interface area between foxe3:GFP+ cells and rx2:H2B-RFP+ cells?*

That is for sure an interesting question. We are aware of this population of cells. We currently do not have data that clarify the fate of those cells with the required certainty. Rather than speculating, we are currently following up on that question by scRNA sequencing, however we see that beyond the scope of the current manuscript.

> *(5) Fig. 5e indicates the depth of Rx3 expression at day 1. Is the depth the thickness of Rx3 expressing cell sheet, which covers the central lens core in the organoids? If so, I wonder if total cell number of Rx3 expressing cell sheet may be different in each seeded-cell number, because thickness is the same across each seeded-cell number, but the surface area size may be different depending on underneath the lens core size. Please clarify this point.*

The referee is right, figure 5e indicates the thickness of the cell sheet expressing Rx3 positioned at the surface of the organoid. Indeed, the number of Rx3-expressing cells (and lens cells) scales with the size of the organoid as stated in the submitted manuscript. We have taken care to remove ambiguities related to that point in the revised version of the manuscript.

> *(6) Noggin application inhibits lens formation at day 0-1. BMP signaling regulates formation of lens placode and olfactory placode at the early stage of development. It is interesting to examine whether Noggin-treated organoid expands olfactory placode area. Please check forebrain territory markers.*

What tissue differentiates at the expense of the lens in BMP inhibitor-treated organoids is of course an intriguing question.

To address this point, we labeled Noggin treated organoids at day 2 and day 3 with forebrain and olfactory placode markers. We could identify an increase in the domains expressing Lhx2, HuC/D and Otx2 in Noggin-treated organoids, showing a shift of the preferential differentiation of the neurons of anterior forebrain identity (see attached figure for reviewer). However, the available markers Lhx2, HuC/D and Otx2 found in the olfactory placode are in addition also co-expressed in further neuronal cell types of the anterior forebrain. While the speculation is tempting, the shift in expression does not allow to conclusively state the expansion of the olfactory placode.

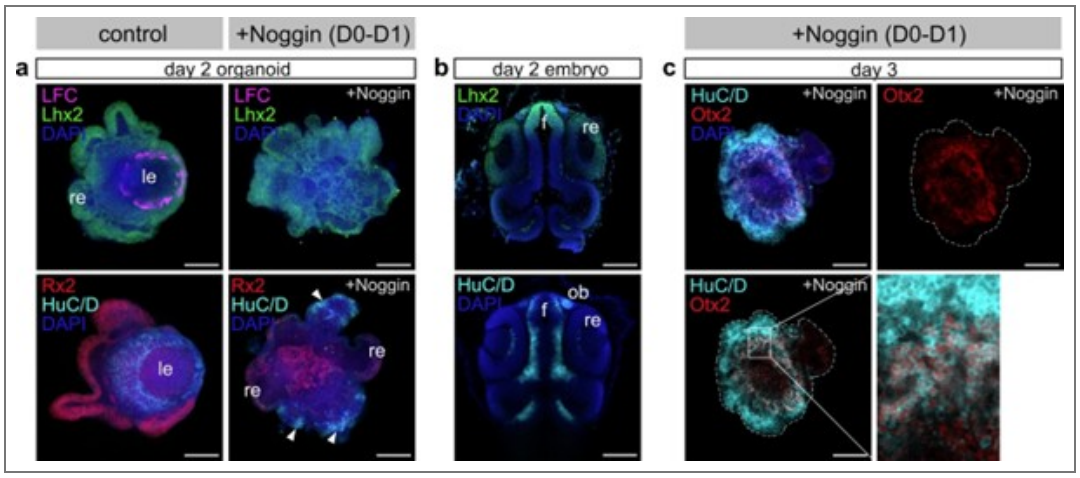

Author response image 1. **Expression of forebrain and olfactory placode markers.**

I have no minor comments

Referees cross-commenting

I agree that all reviewers have similar suggestions, which are reasonable and provided the same estimated time for revision.

Reviewer #1 (Significance):

Strength:

This study is unique. The authors examined eye cup morphogenesis using fish retinal organoids. Eye cup normally consists of the lens, the neural retina, pigment epithelium and optic stalk. However, retinal organoids seem to be simple and consists of two cell types, lens and retina. Interestingly, a similar optic cup-like structure is achieved in both cases; however, underlying mechanism is different. It is interesting to investigate how eye morphogenesis is regulated in retinal organoids,under the unconstrained embryo-free environment.

Limitation:

Description is OK, but analysis is not much profound. It is necessary to apply a bit more molecular and cellular level analysis, such as tracking of cell movement and visualization of FGF signaling in organoid tissues.

Advancement:

The current study is descriptive. Need some conceptual advance, which impact cell biology field or medical science.

Audience:

The target audience of current study are still within ophthalmology and neuroscience community people, maybe translational/clinical rather than basic biology. To beyond specific fields, need to formulate a general principle for cell and developmental biology.

Reviewer #2 (Evidence, reproducibility and clarity):

In this study from Stahl et al., the authors demonstrate that medaka pluripotent embryonic cells can self-organise into eye organoids containing both retina and lens tissues. While these organoids can self-organize into an eye structure that resembles the

> *vertebrate eye, they are built from a fundamentally different morphogenetic process - an "inside-out" mechanism where the lens forms centrally and moves outward, rather than the normal "outside-in" embryonic process. This is a very interesting discovery, both for our understanding of developmental biology and the potential for tissue engineering applications. The study would benefit from some additional experiments and a few clarifications.*
>
> *The authors suggest that the lens cells are the ones that move from the central to a more superficial position. Is this an active movement of lens cells or just the passive consequence of the retina cells acquiring a cup shape? Are the retina cells migrating behind the lens or the lens cells pushing outwards? High-resolution imaging of organoid cup formation, tracking retina cells in combination with membrane labeling of all cells would help elucidate the morphogenetic processes occurring in the organoids. Membrane labeling would also be useful as Prox1 positive lens cells appear elongated in embryos while in the organoids, cell shapes seem less organised, less compact and not elongated (for example as shown in Fig 3f,g).*

Looking into the detail of how the optic cup-like arrangement of ocular organoids is achieved on the cellular level is indeed highly interesting. In the revised manuscript we now provide evidence that the formation of cup-like structure of the ocular organoids presented here is mediated by the following processes: establishment of retina and lens domains at distinct regions of the organoid – retina on the surface and lens in the center (see Figure 3-figure supplement 1d and Figure 3e, and Figure 4). Further, the dislocation of the centrally formed lens towards the organoid periphery results in the opening of the retina layer, moving the lens to the periphery while retinal cells stay static. We propose that the cup-like shape is acquired by an extrusion process of the lens from the center of the organoid.

To address cellular mechanisms involved in this process, we included additional experiments and followed the movements of retinal and lens cells (see new Figure 4c and 4e, new Videos S6, S7 and S8).

Retinal cells (tracked as nuclei of the Rx3::H2B-GFP transgenic line) display repeated short distance movements within the retinal epithelium. These movements are characteristic for interkinetic nuclear migration as found in the developing retina.

In contrast, Foxe3::GFP lens progenitor cells performed long distance movements from the center to the periphery of the organoid. This movement was accompanied by profound cell shape changes of lens progenitor cells, suggesting an active movement of lens cells to the organoid periphery.

These movements are shown in new/extended figures and in new supplementary videos (new Figure 4c and 4e, new Videos S6, S7 and S8) in the revised version of the manuscript.

> *The organoids could be a useful tool to address how cell fate is linked to cell shape acquisition. In the forming organoids, retinal tissue initially forms on the outside, while non-retinal tissue is located in the centre; this central tissue later expresses lens markers. Do the authors have any insights into why fate acquisition occurs in this pattern? Is there a difference in proliferation rates between the centrally located cells and the external ones? Could it be that highly proliferative cells give rise to neural retina (NR), while lower proliferating cells become lens?*

We agree with the reviewer that this is a highly interesting question and in the revised manuscript we followed the advice and dedicated a part of the discussion to this topic. We believe that the arrangement is due to the induction of central lens fates by signal emanating from the retinal epithelium and discuss the role of the diffusion limit and the potential contribution of BMB and FGF signaling to this arrangement. Additional experiments

addressing the target tissues of FGF and BMP signaling in the organoid have been provided in response to Reviewer #1. Interfering with FGF signaling that is essential for lens fiber cell differentiation interestingly did not impact on the lens size arguing against an immediate proliferative effect. Although the analysis of the respective proliferation rates at the surface or in the central region of the organoid might show some differences, we do not have any indications, that the proliferation rate itself would be instructive or superior to the cell fate decisions.

> *What happens in organoids that do not form lenses? Do these organoids still generate foxe3 positive cells that fail to develop into a proper lens structure? And in the absence of lens formation, does the retina still acquire a cup shape?*

Lens formation is primarily dependent on the acquisition/specification of Foxe3-expressing lens placode progenitors. In the absence of Foxe3-expression, a lens does not develop. Once Foxe3-expressing progenitors are established, a lens is formed in unperturbed conditions (measured by the presence of expression of crystallin proteins). Organoids that do not have a lens, do not contain Foxe3-expressing cells.

In the absence of a lens, the organoid is composed of retinal neuroepithelium, that does not form an optic cup like shape (for details of such phenotypes please see Zilova et al., 2021, eLIFE). We took care to state that clearly in the revised manuscript.

> *The author suggest that lens formation occurs even in the absence of Matrigel. Is the process slower in these conditions? Are the resulting organoids smaller? While there are indeed some LFC expressing cells by day2, these cells are not very well organised and the pattern of expression seems dotty. Moreover, LFC staining seems to localise posterior to the LFC negative, lens-like structure (e.g. Fig.S1 3o'clock). How do these organoids develop beyond day 4? Do they maintain their structural integrity at later stages?*
>
> *The role of HEPES in promoting organoid formation is intriguing. Do the authors have any insights into why it is important in this context? Have the authors tried other culture conditions and does culture condition influence the morphogenetic pathways occurring within the organoids?*

We thank the reviewer for pointing this out. In the revised manuscript we made sure to be sufficiently clear in the wording and description of our observation. Indeed, Matrigel is not required for the acquisition of lens fate, which can be demonstrated by the expression of lensspecific markers. However, the presence of Matrigel has a profound impact on structural aspects of organoid formation. Matrigel is essential for organization of retinal-committed cells to form a retinal epithelium (Zilova et al., 2021, eLife). The absence of the structure of the retinal epithelium indeed negatively impacts on the cellular organization and the overall lens structure.

To clarify the contribution of the Matrigel to the organoid organization, we performed additional experiments (see revised Figure 2-figure supplement 1c-f). As mentioned above, the absence of Matrigel impacts on the organization and thickness of retinal neuroepithelium ($Rx2^+$, Figure 2-figure supplement 1c). However, measurement of the lens in organoids at day 2 and day 5 showed that size of the lens is not impacted upon in the absence of Matrigel (Figure 3-figure supplement 1d-e). Additionally, taking advantage of the Foxe3::GFP lens reporter line, we measured the onset of lens-specific gene expression in organoids with and without Matrigel. In both conditions, with and without Matrigel supplementation, Foxe3::GFP expression was initiated at 25 hours post aggregation (see revised Figure 4b).

The role of the HEPES in lens formation is indeed very intriguing and currently under investigation. HEPES is mainly used to regulate the pH of the culture media which on its own might have an impact on multiple cellular processes. It will require a significant time

investment to address the potential HEPES triggered molecular mechanisms impacting on lens formation (cross reference with Reviewer #3), which goes beyond the scope of the current manuscript.

> *Referees cross-commenting*
>
> *Pleased to see that all the other reviewers are positive about the study and raise similar concerns and comments*
>
> ***Reviewer #2 (Significance):***
>
> *This is a very interesting paper, and it will be important to determine whether this alternative morphogenetic process is specific to medaka or if similar developmental routes can be recapitulated in organoid cultures from other vertebrate species.*
>
> ***Reviewer #3 (Evidence, reproducibility and clarity):***
>
> *Summary:*
>
> *The manuscript by Stahl and colleagues reports an approach to generate ocular organoids composed of retinal and lens structures, derived from Medaka blastula cells. The authors present a comprehensive characterisation of the timeline followed by lens and retinal progenitors, showing these have distinct origins, and that they recapitulate the expression of differentiation markers found in vivo. Despite this molecular recapitulation, morphogenesis is strikingly different, with lens progenitors arising at the centre of the organoid, and subsequently translocating to the outside.*
>
> *Comments:*
>
> *The manuscript presents a beautiful set of high quality images showing expression of lens differentiation markers over time in the organoids. The set of experiments is very robust, with high numbers of organoids analysed and reproducible data. The mechanism by which lens specification is promoted in these organoids is, however, poorly analysed, and the reader does not get a clear understanding of what is different in these experiments, as compared to previous attempts, to support lens differentiation. There is a mention to HEPES supplementation, but no further analysis is provided, and the fact that the process is independent of ECM contradicts, as the authors point out, previous reports. The manuscript would benefit from a more detailed analysis of the mechanisms that lead to lens differentiation in this setting.*

We followed the reviewer's advice and have included a systematic analysis of the contribution of ECM (Matrigel) to the process of lens formation. In the revised manuscript we made sure to be sufficiently clear in the wording and description of our observation. Indeed, Matrigel is not required for the acquisition of lens fate, which can be demonstrated by the expression of lensspecific markers. However, the presence of Matrigel has a profound impact on structural aspects of organoid formation. Matrigel is essential for organization of retinal-committed cells to form a retinal epithelium (Zilova et al., 2021, eLIFE). The absence of the structure of the retinal epithelium in turn indeed negatively impacts on the cellular organization and the overall lens structure.

To clarify the contribution of the Matrigel to the organoid organization, we performed additional experiments (see revised Figure 2-figure supplement 1c-f). As mentioned above, the absence of Matrigel impacts on the organization and thickness of retinal neuroepithelium ($Rx2^+$, Figure 2-figure supplement 1c). However, measurement of the lens in organoids at day 2 and day 5 showed that size of the lens is not impacted upon by the absence of Matrigel (Figure 3-figure supplement 1d-e).

Additionally, taking advantage of the Foxe3::GFP lens reporter line, we measured the onset of lens-specific gene expression in organoids with and without Matrigel. In both conditions (with and without Matrigel supplementation), Foxe3::GFP expression was initiated at 25 hours post aggregation (see revised Figure 4b).

The role of the HEPES in lens formation is indeed intriguing and currently under investigation. HEPES is mainly used to adjust the pH of the culture media, which, on its own might have an impact on multiple cellular processes. It will require a significant time investment to address the potential HEPES triggered molecular mechanisms impacting on lens formation (cross reference with Reviewer #3), which clearly goes beyond the scope of the current manuscript.

> *The markers analysed to show onset of lens differentiation in the organoids seem to start being expressed, in vivo, when the lens placode starts invaginating. An analysis of earlier stages is not presented. This would be very informative, allowing to determine whether progenitors differentiate as placode and neuroepithelium first, to subsequently continue differentiating into lens and retina, respectively. Could early placodal and anterior neural plate markers be analysed in the organoids? This would provide a more complete sequence of lens vs retina differentiation in this model.*

We have taken care to show according stages in embryo and organoid side by side. We provide additional data to highlight the expression of Rx3::H2B-GFP (retina) and Foxe3::GFP (lens and lens placode) markers in earlier developmental stages. For the presumptive eye field within the region of the anterior neural plate (S16, late gastrula) Rx3 represents one of the earliest markers (see revised Figure 3-figure supplement 1). Already before an apparent lens placode is formed (see revised Figure 3d) Foxe3::GFP expression is detected within the presumptive lens ectoderm, demonstrating that Foxe3 is ideally suited as an early marker for placodal progenitors in medaka. The onset of Rx3 and Foxe3-driven reporters is clearly early enough to support the claim about the separate origin of the lens (placodal) and retinal (anterior neuroectoderm) tissues within the ocular organoids now represented in the revised figures.

> *The analysis of BMP and Fgf requirement for lens formation and differentiation is suggestive, but the source of these signals is not resolved or mentioned in the manuscript. Are BMP4 and Fgf8 expressed by the organoids? Where are they coming from?*

Assessing the activity of BMP and FGF signaling (cross-reference to Reviewer #1) in the organoids is an important point that we have taken care of and included in the revised manuscript.

To address this point, we assessed which tissue/part of the organoid is responding to BMP and FGF signaling. To do so we analyzed the presence of phosphorylated SMAD1/5/8 (pSMAD1/5/8) and phosphorylated ERK (pERK1/2) as BMP and FGF signaling target in ocular organoids from day 1 to day 2. BMP signaling activity was detected in the center (region of establishment of lens-committed progenitors (Figure 3e)) of the organoid at day 1 (see revised Figure 6a). At day 1, only low levels of FGF signaling activity were detectable in presumptive retinal or/and lens tissue (see revised Figure S6b). Only half a day later, a significant increase in FGF activity was observed specifically in the central region of the organoids (lens progenitor domain, at day 1.5), prior to the onset of differentiation of lens fiber cells. This, together with inability of lens progenitor cells to differentiate to lens fiber cells in the presence of FGF inhibitor SU5402 provided during this critical period (day 1 to day 2) demonstrates that FGF signaling activity localized in the lens progenitor cells is required for lens fiber differentiation.

By day 2, FGF activity was detected in both lens and retinal tissue of the organoid. Similar

patterns of FGF activity were observed in embryos at 2 days post fertilization (see revised Figure S6b).

The treatment with the FGF signaling inhibitor SU5402 from day 0 to day 1 did have no impact on the core size of organoid the dimension of which were fully comparable to the control (please see Figure 6b).

Related to the presence of the corresponding ligands we can state that they are indeed expressed in the organoids at the matching stages based on RNA seq and RT-PCR analyses, however we could not find them specifically localized. This may be due to a widespread, ubiquitous expression or may simply relate to technical problems.

While we can state with confidence that the ligands are present at the relevant time points and trigger the downstream pathways in a localized manner, the question whether the response is due to a localized signal or localized competence remains to be addressed.

> *The fact that the lens becomes specified in the centre of the organoid is striking, but it is for me difficult to visualise how it ends up being extruded from the organoid. Did the authors try to follow this process in movies? I understand that this may be technically challenging, but it would certainly help to understand the process that leads to the final organisation of retinal and lens tissues in the organoid. There is no discussion of why the morphogenetic mechanism is so different from the in vivo situation. The manuscript would benefit from explicitly discussing this.*

Following the shift of the lens in vivo is indeed very relevant suggestion and we have taken care to address this in the revised manuscript.

To clarify this process, we included additional experiments and followed the movements of lens cells (see new Figures 4c, 4d and 4e, new Videos S6 and S7). Foxe3::GFP lens progenitor cells were found to actively move over long distances from center to the organoid periphery. This movement was accompanied by profound cell shape changes of lens progenitor cells with the active extension of lamellipodia and filopodia strongly arguing for an active movement of lens cells to the organoid periphery (cross-reference with Reviewer #1 and Reviewer #2).

> *Referees cross-commenting*
>
> *We all seem to have similar comments and concerns. I think overall the suggestions are feasible and realistic for the timeframe provided.*
>
> ***Reviewer #3 (Significance):***
>
> *This study describes a reproducible approach to differentiate ocular organoids composed of lens and retinal tissues. The characterisation of lens differentiation in this model is very detailed, and despite the morphogenetic differences, the molecular mechanisms show many similarities to the in vivo situation. The manuscript however does not highlight, in my opinion, why this model may be relevant. Clearly articulating this relevance, particularly in the discussion, will enhance the study and provide more clarity to the readers regarding the significance of the study for the field of organoid research, ocular research and regenerative studies.*

https://doi.org/10.7554/eLife.108702.2.sa0